SORPTION, ION EXCHANGE AND EQUILIBRIUM CHEMISTRY IN ADVECTIVE-DISPERSIVE SOLUTE TRANSPORT

by

Frank Murray Lewis

A Thesis Submitted to the Faculty of the

DEPARTMENT OF HYDROLOGY AND WATER RESOURCES

In Partial Fulfillment of the Requirements
For the Degree of

MASTER OF SCIENCE
WITH A MAJOR IN HYDROLOGY

In the Graduate College

THE UNIVERSITY OF ARIZONA

1 9 8 4

STATEMENT BY AUTHOR

This thesis has been submitted in partial fulfillment of the requirements for an advanced degree at the University of Arizona and is deposited in the University Library to be made available to borrowers under rules of the Library.

Brief quotations from this thesis are allowable without special permission, provided that accurate acknowledgement of source is made. Requests for permission for extended quotation from or reproduction of this manuscript in whole or in part may be granted by the head of the major department or the Dean of the Graduate College when in his judgment the proposed use of the material is in the interests of scholarship. In all other instances, however, permission must be obtained from the author.

SIGNED: Frank Murray Lewis

APPROVAL BY THESIS DIRECTOR

This thesis has been approved on the date shown below:

Shlomo Neuman

S. P. NEUMAN
Professor of Hydrology and
Water Resources

11/29/84
Date

ACKNOWLEDGMENTS

My completion of this thesis was greatly facilitated by the help guidance and support of several people. Dr. Clifford Voss of the U.S. Geological Survey suggested the topic and provided his as yet unpublished transport code upon which a large portion of this thesis is based. In addition, he contributed invaluable assistance in developing the basic model structure and funded the necessary computer facilities. For all his help, support and friendship, I am especially grateful. I am also very grateful to Dr. Shlomo Neuman whose courses provided the impetus for me to pursue research in ground-water modeling and who offered valuable suggestions on this manuscript in his role as committee chairman. To the other members of my committee, Drs. Eugene S. Simpson and Soroosh Sorooshian, I am thankful for their assistance.

I must thank Dr. Jacob Rubin of the U.S. Geological Survey who developed the reactive transport mathematics and provided some of the example problems used to test the model. His comments and suggestions throughout the course of this study were most appreciated. My wife, Panagiota, did all the graphic line work and offered valuable assistance in the layout and presentation of all figures. She also deserves special thanks for very kindly tolerating the lifestyle that only the wife of a graduate student knows. I am very grateful for her patience, confidence and support.

The final copy of this thesis may never have been completed without Joanne Taylor who helped me tremendously with her word-processing expertise and generously volunteered her time; Joanne, thank you. Last, but most certainly not least, I wish to extend my deepest appreciation to my parents for all the support and confidence they have given me over the years.

TABLE OF CONTENTS

TABLE OF CONTENTS--Continued

LIST OF ILLUSTRATIONS

LIST OF ILLUSTRATIONS--Continued

LIST OF ILLUSTRATIONS--Continued

LIST OF TABLES

ABSTRACT

A method of incorporating specific classes of generic chemical reactions into advective-dispersive solute transport is presented. The reactions comprise a hybrid system governed by local chemical equilibrium in which both solute-solid and homogeneous aqueous interactions occur simultaneously. The chemical environment may be defined either by the linear sorption of a single species and two soluble complexation reactions which also involve that species, or binary ion exchange and one complexation reaction involving a common ion. In each case, a total of three solutes are transported. A set of three partial differential equations is developed, only one of which is nonlinear. These equations are solved numerically in two dimensions through the modification of an existing finite-element ground-water flow/transport algorithm. Example runs are presented that demonstrate the individual and combined effects of linear sorption, ion exchange and aqueous reactions on the simultaneous transport of several solutes in chemical equilibrium.

INTRODUCTION

The traditional approach to modeling problems of ground-water contamination involve a numerical solution to the advection-dispersion equation describing the transport of a single, nonreactive, solute (e.g., Bredehoeft and Pinder, 1973; Pinder, 1973; Konikow and Bredehoeft, 1974). Additionally, several investigators (e.g., Holly and Fenske, 1968; Lai and Jurinak, 1972; Gupta and Greenkorn, 1973; Pickens and Lennox, 1976) have incorporated solute-porous media interactions through a source/sink term in their respective mass-balance equations. Consequently, mechanisms such as adsorption and ion exchange have been accounted for, adding an additional level of complexity to single-solute transport.

Problems posed in natural systems, however, frequently involve several solutes that not only interact with the porous media, but among themselves. Investigations of multicomponent reactive transport are not new. Solution techniques have been developed since the early 1970's that account for multiple solutes participating in various chemical reactions. Jennings et al. (1982) and Miller and Benson (1983) have noted that two fundamentally different approaches have been applied to simulate chemically active transport. The first approach separates the partial differential equations used to describe the physical mass balance of each solute from the algebraic expressions that define various chemical processes such as sorption isotherms and chemical equilibria.

The solution is obtained by iterating between the two sets of equations: solving first for physical transport alone, followed by the simulation of chemical interaction until a new equilibrium is reached. This "two-step" procedure has been employed in studies by Lake and Helfferich (1978), Grove and Wood (1979), and Cederberg et al. (1984) among others. The approach is potentially very powerful especially when combined with available computer codes such as WATEQF (Plummer et al., 1978) and PHREEQE (Parkhurst et al., 1982) which facilitate equilibrium calculations for large chemical systems.

The principal disadvantages of this method have been outlined by Jennings et al. (1982). They report difficulty in obtaining convergent solutions when iterating between the two types of equation sets, and note that the mechanics of this iteration process have been analyzed only recently. Another disadvantage arises when the chemical equilibria models such as those mentioned above are employed. These computer codes are large in order to be general, and may not be highly efficient inasmuch as the solution of each run represents equilibrium in a physically static system. Their use in conjunction with transport studies, where the equilibrium code must be activated once for each node, on every iteration, and for all time steps, may lead to excessive computer time requirements.

The second approach involves a single equation set in which the chemical processes have been directly incorporated into the mass-balance equations. This usually leads to a set of nonlinear partial differential equations that may be solved simultaneously in a "one-step"

procedure. Success folowing this general approach has been reported by several investigators.

The first such study was a comprehensive analysis of ion exchange in multisolute dispersive transport by Rubin and James (1973). They arrived at a set of coupled nonlinear partial differential equations that represent a general multispecies system under a local chemical equilibrium constraint. A Galerkin finite-element model was developed to solve the equation set for steady, one-dimensional flow in saturated porous media. The model was used to examine the effects of homogeneous as well as layered media, variable total dissolved solute concentration, selectivity coefficients as both a constant and a function of concentration, and multicomponent exchange.

Valocchi et al. (1981) developed an analytical methodology based on chromatography that attempts to characterize multiple fronts and plateau zones typically observed in some cases of transport with ion exchange (e.g., Rubin and James, 1973; Grove and Wood, 1979). The paper advanced previous chromatographic studies applied in the soil sciences to include heterovalent exchange and variable total solute concentration. In addition, a field problem was simulated in two dimensions to test the chromatographic theory at a larger scale. Their study followed essentially the same transport-equation development, and employed a similar numerical solution technique as that of Rubin and James (1973).

The one-step approach has also been employed by Jennings et al. (1982). They addressed soluble complexation as well as linear, nonlinear and competitive nonlinear sorption in conjunction with a chemical

transport system containing an arbitrary number of components. By allowing for the sorption of several species, and for arbitrary stoichiometric coefficients, their method produced a set of partial differential equations, each of which may be strongly nonlinear. A Galerkin finite-element model was developed to solve the equation set in one dimension, and to present examples that demonstrate the effect of complexation on the transport of sorbing species.

Miller and Benson (1983) recently developed a model to simulate ion exchange and soluble complexation, along with the dissociation of water in multisolute dispersive transport. Unlike previous one-step procedures, a fully implicit finite-difference scheme was used together with chemical-relation equations to formulate a set of algebraic/differential equations. These equations, in turn, were incorporated into a single, general, matrix equation in which the vector of dependent variables may contain several different unknowns for each node. Solutions for all unknown concentrations were subsequently obtained simultaneously using Newton-Raphson iterations. Although apparently well suited for chemical systems containing several multiple-component reactions, a trade off must be made between the number of transported solutes and the number of nodes required to define a given problem adequately.

This thesis details the development of a new model, SATRA-CHEM, which combines the mathematical principles of specific classes of generic chemical reactions developed by Rubin (1983a, 1983b, 1984) with an existing finite-element solute-transport model, SATRA, developed by

Voss (n.d.). The new model follows the concept of the one-step approach discussed above; however, it differs in the way the mathematics of transport and associated chemical reactions are linked in a physically natural way. Rubin (1983a) has demonstrated that the manner in which reactive-solute transport problems are formulated mathematically, depends on the nature of the chemical processes involved.

This study employs a general formulation which facilitates the analysis of transported solutes that simultaneously participate in both equilibrium-controlled aqueous reactions and either linear sorption or binary ion exchange. The inherent nonlinear components resulting from these combined chemical processes are reduced into two time-dependent variables that essentially plug into a general form of the classic advection-dispersion equation. The resulting equation is directly compatible with the two-dimensional transport algorithm applied in SATRA and, potentially, other existing codes as well.

SOLID PHASE INTERACTION IN SOLUTE TRANSPORT

SATRA-CHEM is a modified version of the existing computer code SATRA that has been altered to incorporate multiple solutes and chemical interactions. SATRA is a two-dimensional finite-element model which is capable of simulating both ground-water flow and constant-density solute transport. The method through which the model obtains hydraulic heads, however, is not discussed in this thesis. A complete description of the flow equation and its solution by SATRA may be found in Voss (n.d.).

SATRA-CHEM solves the advection-dispersion equation for fully saturated, heterogeneous porous media which may be anisotropic with respect to hydraulic conductivity, and assumes dispersivities are direction-independent. The general form of this equation may be written in terms of a dissolved concentration, C, as

$$\frac{\partial(\varepsilon C)}{\partial t} = \underline{\nabla}\cdot(\varepsilon \underline{\underline{D}}\cdot\nabla C) - \underline{\nabla}\cdot(\varepsilon \underline{v} C) - f + QC^{*} \qquad (1)$$

where

$\underline{\nabla}$ = a 2-D differential operator [1/L]

ε = porosity [1]

C = solute concentration [M/L^3]

$\underline{\underline{D}}$ = dispersion tensor [L^2/t]

$\underline{v}$ = average fluid velocity [L/t]

f = adsorbate source [M/tL^3]

Q = volumetric fluid source [1/t]

C^{*} = solute concentration of fluid source [M/L^3]

A listing of all variables and notation used in this thesis may be found in Appendix A.

The principal difference between the model SATRA and its modified version SATRA-CHEM, is the ability of the latter to simulate the effects of f in equation (1). The term f denotes the transfer of solute mass from solution onto the solid surface as adsorbate, and hence may be viewed as an adsorbate source. In general, f is a function of solute concentration, adsorbate concentration, and the rate of change in solute concentration, depending on the appropriate sorption isotherm. These factors are quantified in the fundamental form of the transport equation solved by SATRA-CHEM.

To arrive at this form, the adsorbate source may be written in terms of bulk density (ρ_b) and an adsorbate flux (f_s) as

$$f = \rho_b f_s \tag{2}$$

The adsorbate flux represents the solute-mass adsorption rate per unit mass of solid matrix [$(M/M_s)/t$], and may be expanded into a general form as

$$f_s = k_1 \frac{\partial U}{\partial t} + k_2$$

such that the mechanisms of linear sorption or binary ion exchange are accommodated through the coefficients k_1 [L^3/M_s] and k_2 [$(M/M_s)/t$]. As will be shown below, these coefficients may also account for aqueous interaction among dissolved solutes when such reactions accompany these sorptive processes. Consequently, these coefficients are defined in the next chapter according to the nature of the chemical interaction.

The adsorbate source may now be expressed in general as

$$f = (1-\varepsilon)\rho_s \left(k_1 \frac{\partial C}{\partial t} + k_2\right) \tag{3}$$

where ρ_s is the solid-grain density $[M_s/L^3]$. Substituting (3) into (1) and rearranging, results in

$$\frac{\partial(\varepsilon C)}{\partial t} + [(1-\varepsilon)\rho_s k_1]\frac{\partial C}{\partial t} - \underline{\nabla}\cdot(\varepsilon \underline{\underline{D}}\cdot\underline{\nabla}C) + \underline{\nabla}\cdot(\varepsilon \underline{v} C) = QC^* - (1-\varepsilon)\rho_s k_2 \tag{4}$$

Further modification of the transport equation into the form solved by the model requires the concept of mass-conservative solute balance to be introduced (Voss, n.d.). At present, equation (4) contains redundant expressions for the time rate-of-change in solute mass per unit total solid matrix volume due to the way in which the head solutions are obtained prior to transport. The flow simulation is performed basically through a fluid-mass balance at every point in the ground-water system. In its most fundamental form this fluid-mass balance is defined on a per unit volume basis as

$$\frac{\partial(\varepsilon\rho)}{\partial t} = -\underline{\nabla}\cdot(\varepsilon\rho\underline{v}) + Q\rho \tag{5A}$$

where ρ is the fluid density. An important factor in determining the amount of total fluid mass in a unit volume of porous media is the temporal change in the storage capability of the media due to fluctuations in hydraulic head. If the fuid density is assumed to remain constant, this factor is implicitly accounted for in the mass-balance relationship (5A) when that expression is multiplied by concentration, C. The resulting product represents the changes in solute mass caused by variations in fluid mass within a unit volume of porous media:

$$C \frac{\partial(\varepsilon)}{\partial t} + C\underline{\nabla}\cdot(\varepsilon\underline{v}) = QC \qquad (5B)$$

When (5B) is subtracted from equation (4), the redundant mass-balance information is eliminated and the result is

$$[\varepsilon + (1-\varepsilon)\rho_s k_1] \frac{\partial C}{\partial t} - \underline{\nabla}\cdot(\varepsilon\underline{\underline{D}}\cdot\underline{\nabla}C) + \varepsilon\underline{v}\cdot\nabla C = Q(C^*-C)-(1-\varepsilon)\rho_s k_2$$

For simplicity, the principal advective-dispersive components may be lumped together into the following two-dimensional differential operator:

$$L(C) = \underline{\nabla}\cdot(\varepsilon\underline{\underline{D}}\cdot\underline{\nabla}C) - \varepsilon\underline{v}\cdot\underline{\nabla}C \qquad (6)$$

Using this relationship, the final general form of the solute-transport equation solved by the model may be written as

$$[\varepsilon + (1-\varepsilon)\rho_s k_1] \frac{\partial C}{\partial t} = L(C) + Q(C^*-C) - (1-\varepsilon)\rho_s k_2 \qquad (7)$$

CHEMICAL INTERACTION IN SOLUTE TRANSPORT

The focus of this thesis is on the simultaneous transport of several dissolved constituents. Specifically, the constituents involved are expressed in terms of tenads. In a given chemical system, a tenad is best defined as a chemical entity whose total mass is not influenced by the reaction process, regardless of whether it is an active participant or not. In other words, the total mass of a tenad is always conserved, even if it is sorbed. If a tenad is not sorbed, the definition implies the total dissolved concentration of that tenad is transported as a conservative quantity. Further explanation and specific examples of tenads in chemical systems may be found in Rubin (1983a).

The current version of SATRA-CHEM was developed to simulate the transport of multiple solutes in two different hybrid chemical systems. In the first system, three tenads are allowed to interact through aqueous equilibrium-controlled reactions while one of the three is additionally able to sorb onto the solid matrix. The second system involves four tenads that simultaneously interact through binary ion exchange and an aqueous equilibrium reaction. Both chemical transport systems are solved by the same computer code. The governing equations have exactly the same form, but each system requires a different mathematical analysis to define the coefficients k_1 and k_2 in equation (7).

Assumptions for Reactive Transport

In order to facilitate the demonstration of a general approach to reactive transport, the mathematical formulation employed in this study is based on physical conditions that represent a relatively simple chemical environment. The model assumes isothermal conditions with constant fluid density and viscosity. In addition, the fluid velocity may vary through porous media considered chemically homogeneous in terms of its reactive capabilities. All reactions are assumed to be reversible and sufficiently fast such that local chemical equilibrium is continually maintained. This implies that the reaction rate greatly exceeds the actual physical transport process.

The assumption that local chemical equilibrium prevails is only an approximation of natural systems. In practice, the actual conditions required for instantaneous equilibrium are difficult to determine, and complete equilibrium is rarely attained (Drever, 1982). The issue of whether local equilibrium is an appropriate assumption in modeling reactive solute transport is the subject of recent studies by Valocchi (1984) and Jennings and Kirkner (n.d.).

The alternative to assuming continuous chemical equilibrium is to account for reaction kinetics which is generally both conceptually and mathematically more complex. Nevertheless, methodologies describing transport involving specific classes of reactions that are not governed by local chemical equilibrium have been developed (e.g., Rubin, 1983a).

Further assumptions in this model involve the stoichiometric and activity coefficients all of which, for simplicity, are set equal to

one. The inclusion of values other than one for these coefficients would not involve major programming changes, and future versions of the model may be modified accordingly. Additionally, the chemical equilibrium constants are assumed to be independent of space and time.

Equilibrium Sorption and Aqueous Reactions

Following the notation found in Rubin (1983a), the first system of chemical reactions that the model may simulate individually, or in any simultaneous combination, is:

$$M_1 + \bar{M}_x \rightleftharpoons \overline{M_1 M_x} \qquad \text{(R1)}$$

$$M_1 + M_2 \rightleftharpoons M_1 M_2 \qquad \text{(R2)}$$

$$M_1 + M_4 \rightleftharpoons M_1 M_4 \qquad \text{(R3)}$$

where, M_i i=1,2,3,4 is a dissolved chemical species composed of only one tenad $\{M_i\}$, and $M_i M_j$ i=1, j=2,4 is a dissolved chemical species that contains two tenads $\{M_i\}$ and $\{M_j\}$. $\bar{M}_i$ and $\overline{M_i M_j}$ are the corresponding chemical species in the solid phase, and $\bar{M}_x$ represents the surface of a reactive solid grain. The odd and even nature of the subscripts denotes opposite electrical charges on the chemical components. For reference, even subscripted tenads may be viewed as anions and odd numbered ones as cations. The mathematical theory, however, is independent of these designations.

The concentration of each chemical species in solution will be designated C_i (e.g., moles per unit volume of fluid) for M_i, and C_{ij} for $M_i M_j$. Accordingly, adsorbate concentrations (e.g., moles per unit mass of solids) will be referred to as $\bar{C}_i$ and $\bar{C}_{ij}$.

Reaction R1 describes the sorption of M_1 from solution onto the surface of the solid matrix and, thus, is considered a surface-heterogeneous reaction (Rubin, 1983a). Reactions R2 and R3, on the other hand, occur entirely in the aqueous phase and are, therefore, considered homogeneous reactions. Reactions of this latter sort may describe such processes as complexation, dissociation, oxidation or reduction. In addition, reactions R2 and R3 each have an associated thermodynamic equilibrium constant which may be defined respectively as

$$K_{12} = \frac{C_{12}}{C_1 C_2} \tag{8}$$

$$K_{14} = \frac{C_{14}}{C_1 C_4} \tag{9}$$

Development of Governing Transport Equations

Reactions R1 through R3 are incorporated into expressions of advective-dispersive transport through the procedure outlined below. The result is a set of partial differential equations that are identical in form with equation (7). The first step is to define the basic mass-balance relationships, using the differential operator (6), that describe the two-dimensional transport of each of the three tenads: for $\{M_1\}$,

$$\varepsilon\frac{\partial C_1}{\partial t} + \varepsilon\frac{\partial C_{12}}{\partial t} + \varepsilon\frac{\partial C_{14}}{\partial t} + \rho_b\frac{\partial \bar{C}_1}{\partial t} =$$

$$L(C_1 + C_{12} + C_{14}) + Q(C_1^* + C_{12}^* + C_{14}^* - C_1 - C_{12} - C_{14}) \tag{10}$$

for $\{M_2\}$,

$$\varepsilon\frac{\partial C_2}{\partial t} + \varepsilon\frac{\partial C_{12}}{\partial t} = L(C_2 + C_{12}) + Q(C_2^* + C_{12}^* - C_2 - C_{12}) \qquad (11)$$

and for $\{M_4\}$,

$$\varepsilon\frac{\partial C_4}{\partial t} + \varepsilon\frac{\partial C_{14}}{\partial t} = L(C_4 + C_{14}) + Q(C_4^* + C_{14}^* - C_4 - C_{14}) \qquad (12)$$

These three equations, along with the two reaction quotients (equations (8) and (9)), comprise the basic set of mathematically "mixed" equations from which the five unknown dissolved concentrations are determined (Rubin, 1983a). The term, mixed, refers to the inclusion of both algebraic and partial differential equations within the set.

In order to solve each partial differential equation for a single unknown, the dependent variables may be conveniently represented by the total dissolved concentration of the tenad in question. These new variables are designated U, V and W, where

$$U = C_2 + C_{12} \qquad (13)$$

$$V = C_4 + C_{14} \qquad (14)$$

$$W = C_1 + C_{12} + C_{14} \qquad (15)$$

Source concentrations are designated similarly using the superscript, *. By substituting the relations (13), (14) and (15) into equations (11), (12) and (10) respectively, the transport equations can be expressed more simply in terms of the concentrations U, V and W as

$$\varepsilon\frac{\partial W}{\partial t} + \rho_b\frac{\partial \bar{C}_1}{\partial t} = L(W) - Q(W^* - W) \qquad (16)$$

$$\varepsilon\frac{\partial U}{\partial t} = L(U) - Q(U^* - U) \qquad (17)$$

$$\varepsilon\frac{\partial V}{\partial t} = L(V) - Q(V^* - V) \qquad (18)$$

The adsorbate contribution, $\rho_b \frac{\partial \bar{C}_1}{\partial t}$, in equation (15) is equivalent to f in equation (1), and can be redefined in the solute phase through the appropriate sorption model. If the sorbed concentration $\bar{C}_1$ is assumed to be a function of the concentration in solution, i.e.,

$$\bar{C}_1 = f(C_1)$$

then it follows that

$$\frac{\partial \bar{C}_1}{\partial t} = \frac{\partial \bar{C}_1}{\partial C_1}\frac{\partial C_1}{\partial t}$$

The derivative $\frac{\partial \bar{C}_1}{\partial C_1}$ mathematically represents the partitioning of M_1 between the sorbed and solute phase, and will be called F in all future references. F directly conforms to various sorption isotherms (Bear, 1979); however, in this study, a linear isotherm is assumed in order to facilitate demonstration and analytical verification. In linear sorption, F is constant and analogous to the equilibrium distribution coefficient, K_d, as defined in Freeze and Cherry (1979) and Reardon (1981) among others, i.e.,

$$F = K_d$$

$$= \frac{\text{mass of solute on solid per unit mass of solid}}{\text{mass of solute per unit volume of water}}$$

$$= \frac{\bar{C}_1}{C_1}$$

With F defined, the adsorbate time derivative can now be expressed simply as

$$\frac{\partial \bar{C}_1}{\partial t} = F\frac{\partial C_1}{\partial t}$$

This allows the transport equation (16) for $\{M_1\}$ to be expressed entirely in terms of aqueous concentrations:

$$\varepsilon\frac{\partial W}{\partial t} + \rho_b F\frac{\partial C_1}{\partial t} = L(W) + Q(W^* - W) \tag{19}$$

In order to solve this equation both derivatives must be in terms of the same concentration variable. $\frac{\partial C_1}{\partial t}$ can be described as a function of $\frac{\partial W}{\partial t}$ by first rearranging the chemical-relation equations (8) and (9) to read:

$$C_{12} = K_{12}C_1C_2 \tag{20}$$

$$C_{14} = K_{14}C_1C_4 \tag{21}$$

Next, by combining (8) with (13), and (9) with (15), the following expressions for C_2 and C_4 are obtained:

$$C_2 = \frac{U}{(1+K_{12}C_1)} \tag{22}$$

$$C_4 = \frac{V}{(1+K_{14}C_1)} \tag{23}$$

The subsequent derivatives of these equations with respect to time yield:

$$\frac{\partial C_2}{\partial t} = \left(\frac{1}{(1+K_{12}C_1)}\right)\frac{\partial U}{\partial t} - \frac{K_{12}U}{(1+K_{12}C_1)^2}\frac{\partial C_1}{\partial t} \tag{24}$$

and

$$\frac{\partial C_4}{\partial t} = \left(\frac{1}{(1+K_{14}C_1)}\right)\frac{\partial V}{\partial t} - \frac{K_{14}V}{(1+K_{14}C_1)^2}\frac{\partial C_1}{\partial t} \tag{25}$$

Similarly, if

$$W = C_1 + C_{12} + C_{14}$$

$$= C_1(1 + K_{12}C_2 + K_{14}C_4)$$

then it follows that

$$\frac{\partial W}{\partial t} = \frac{\partial C_1}{\partial t}(1 + K_{12}C_2 + K_{14}C_4) + C_1K_{12}\frac{\partial C_2}{\partial t} + C_1K_{14}\frac{\partial C_4}{\partial t} \tag{26}$$

Equations (24) through (26) clearly illustrate the origins of the non-linear components that complicate the final form of the transport equation for W. Note without the homogeneous equilibrium reactions, $K_{12} = K_{14} = 0$ and equations (24) through (26) are linear.

The derivation continues by substituting equations (24) and (25) for $\frac{\partial C_2}{\partial t}$ and $\frac{\partial C_4}{\partial t}$ in equation (26), and arriving at

$$\frac{\partial W}{\partial t} = \frac{\partial C_1}{\partial t}H + G \tag{27}$$

where

$$H = 1 + K_{12}C_2 + K_{14}C_4 - \left(\frac{K_{12}}{1+K_{12}C_1}\right)^2 UC_1 - \left(\frac{K_{14}}{1+K_{14}C_1}\right)^2 VC_1 \qquad (28)$$

and

$$G = \left(\frac{K_{12}C_1}{1+K_{12}C_1}\right)\frac{\partial U}{\partial t} + \left(\frac{K_{14}C_1}{1+K_{14}C_1}\right)\frac{\partial V}{\partial t} \qquad (29)$$

Equation (27) may be rewritten explicitly for $\frac{\partial C_1}{\partial t}$ as

$$\frac{\partial C_1}{\partial t} = \frac{1}{H}\frac{\partial W}{\partial t} - \frac{G}{H}$$

which, in turn, may be introduced into equation (19) such that the transport equation for W becomes

$$\varepsilon\frac{\partial W}{\partial t} + \rho_b F[(\frac{1}{H})\frac{\partial W}{\partial t} - \frac{G}{H}] = L(W) + Q(\overset{*}{W} - W)$$

After substituting grain density for bulk density, this equation may be rearranged to read:

$$[\varepsilon + (1-\varepsilon)\rho_s \frac{F}{H}]\frac{\partial W}{\partial t} = L(W) + Q(W^* - W) + (1-\varepsilon)\rho_s \frac{FG}{H} \qquad (30)$$

Equation (30) along with equations (17) and (18) comprise the basic set of transport equations solved by SATRA-CHEM when linear sorption and aqueous equilibrium reactions occur together. All three equations have the same form as the more general equation (7), but are derived specifically to account for the simultaneous reactions R1 through R3. In this case, the coefficients k_1 and k_2 in (7) are both zero for equations (17) and (18), but in equation (30) they are defined through the relationships: $k_1 = F/H$, and $k_2 = -FG/H$. All nonlinear

aspects of the chemical interactions are contained in the variables G and H, and the process of linear sorption is incorporated through F.

Overview of Solution Algorithm

The model first solves the linear transport equations (17) and (18) at the end of a given time step (t^k) for U and V respectively. Equation (30), which is nonlinear due to the variables G and H, is then solved for W at t^k using a 'global' iteration scheme. The term global is used to distinguish this process from a localized Newton-Raphson procedure contained within each iteration.

The first step in solving for W is to determine the values of G and H (equations (28) and (29)) on a given iteration. These variables require U and V at t^k, along with their derivatives with respect to time, and values of C_1, C_2 and C_4. The derivatives are expressed simply as the linear change during the time step (e.g., $\partial U/\partial t = (U^k - U^{k-1})/\Delta t$), and the values of C_1, C_2 and C_4 are obtained from the previous global iteration, or the previous time step if on the first iteration. With F known from the input data, all of the unknowns are accounted for and equation (30) can be solved for W.

Following the calculation of U, V and W, the individual reactant concentrations are obtained by simultaneously solving the algebraic expressions (13) through (15). Subtracting (13) and (14) from (15), and using the relationships (22) and (23), produces a single equation with C_1 as the only unknown:

$$\begin{aligned} W - U - V &= C_1 - C_2 - C_4 \\ &= C_1 - U/(1+K_{12}C_1) - V/(1+K_{14}C_1) \end{aligned} \qquad (31)$$

This equation can be converted into the following cubic expression

$$(K_{12}K_{14})C_1^3 + [K_{12}K_{14}(U+V-W)+(K_{12}+K_{14})]C_1^2 + [1 + K_{12}(U-W) + K_{14}(V-W)]C_1 - W = 0 \qquad (32)$$

which the model solves for C_1 using a Newton-Raphson iteration procedure. This procedure requires the user to supply, at the beginning of each global iteration, an initial guess that is high enough to ensure that the greatest positive root is obtained. A guess on the same order of magnitude as the highest anticipated value of W is adequate. A guess that is too low may cause the Newton-Raphson solution to converge on a negative root; consequently, it is best to aim high. The iterations proceed quickly; so even a poor guess still converges rapidly. Once C_1 is known, C_2 and C_4 can be back-calculated from equations (22) and (23). Note the cubic equation can also be solved directly using a formula; however, the coefficients in equations (32) are sufficiently complex that this does not provide a desirable alternative.

Finally, the most recent value of W is checked against the previous global iteration. If the difference between successive values of W is at every node within a user-set tolerance, the model proceeds to the next time step. If not, another global iteration is required and the solution procedure for W is repeated.

When sorption and aqueous complexations do not occur together the algorithm is simplified considerably. Specifically, without homogeneous aqueous reactions equations (13) through (15) reduce to

$$U = C_2$$

$$V = C_4$$

$$W = C_1$$

and without sorption (either with or without homogeneous reactions), equation (30) becomes

$$\epsilon\frac{\partial W}{\partial t} = L(W) + Q(W^{*}-W)$$

Consequently, in both of these cases the resulting transport equations are linear and no global iteration is required. However, in the latter case involving homogeneous reactions, Newton-Raphson iterations are necessary on each time step an output of the reactant concentrations is desired.

Equilibrium Ion Exchange and Aqueous Reactions

The second chemical environment the model is capable of simulating is represented by the following simultaneous reactions:

$$M_1 + \overline{M_3M_e} \rightleftharpoons \overline{M_1M_e} + M_3 \qquad \text{(R4)}$$

$$M_1 + M_2 \rightleftharpoons M_1M_2 \qquad \text{(R5)}$$

The same notation used in the discussion of R1 though R3 also applies to these reactions. Reaction R4 describes binary exchange between M_1 and M_3 in which a tenad in solution interchanges with another tenad in the sorbed phase. The common factor for both tenads is the cation exchanger, $\bar{M}_e$. Like R1, R4 is a surface heterogeneous reaction, and R5, which is identical to R2, is a homogeneous aqueous reaction (Rubin, 1983a).

The algebraic equations that further define this chemical system are the chemical-relation equations

$$K_{13} = \frac{\bar{C}_1 C_3}{C_1 \bar{C}_3} \tag{33}$$

$$K_{12} = \frac{C_{12}}{C_1 C_2} \tag{34}$$

associated with reactions R4 and R5 respectively, and the exchange capacity of the media

$$\bar{C}_T = \bar{C}_1 + \bar{C}_3 \tag{35}$$

which is assumed constant.

Development of Governing Transport Equations

As in the previous chemical system, the environment defined by R4 and R5 can be combined with advective-dispersive transport to formulate a set of partial differential equations identical in form with equation (7) (Rubin, 1984). In this case, the mass-balance relationships for each of the four tenads are:

for $\{M_1\}$,

$$\varepsilon\frac{\partial C_1}{\partial t} + \varepsilon\frac{\partial C_{12}}{\partial t} + \rho_b\frac{\partial \bar{C}_1}{\partial t} = L(C_1 + C_{12}) + Q(C_1^* + C_{12}^* - C_1 - C_{12}) \tag{36}$$

$\{M_2\}$,

$$\varepsilon\frac{\partial C_2}{\partial t} + \varepsilon\frac{\partial C_{12}}{\partial t} = L(C_2 + C_{12}) + Q(C_2^* + C_{12}^* - C_2 - C_{12}) \tag{37}$$

$\{M_3\}$,

$$\varepsilon\frac{\partial C_3}{\partial t} + \rho_b\frac{\partial \bar{C}_3}{\partial t} = L(C_3) + Q(C_3^* - C_3) \tag{38}$$

and $\{\bar{M}_e\}$,

$$\rho_b\frac{\partial \bar{C}_1}{\partial t} + \rho_b\frac{\partial \bar{C}_3}{\partial t} = 0 \tag{39}$$

These four expressions, together with relationships (33) through (35), comprise the basic set of equations from which the unknown solute concentrations are determined.

The number of mass-balance expressions required to define this system may be reduced by one if equations (36) and (38) are added together. This step also accounts for the relationship in equation (39), and eliminates the adsorbate contribution of $\bar{M}_3$ in the mass balance. The result is an expression containing three unknown solute concentrations:

$\{M_1\}+\{M_3\}$:

$$\varepsilon\frac{\partial C_1}{\partial t} + \varepsilon\frac{\partial C_{12}}{\partial t} + \varepsilon\frac{\partial C_3}{\partial t} =$$

$$L(C_1 + C_{12} + C_3) + Q(C_1^* + C_{12}^* + C_3^* - C_1 - C_{12} - C_3) \tag{40}$$

To facilitate the solution process, the combined aqueous concentrations associated with each differential equation are expressed as a single variable. This allows equations (36), (37) and (40), to be transformed into the following:

$$\varepsilon\frac{\partial W}{\partial t} + \rho_b\frac{\partial \bar{C}_1}{\partial t} = L(W) + Q(W^* - W) \tag{41}$$

$$\epsilon\frac{\partial U}{\partial t} = L(U) + Q(U^* - U) \tag{42}$$

$$\epsilon\frac{\partial V}{\partial t} = L(V) + Q(V^* - V) \tag{43}$$

where

$$W = C_1 + C_{12} \tag{44}$$

$$U = C_2 + C_{12} \tag{45}$$

$$V = C_1 + C_{12} + C_3 \tag{46}$$

$$= W + C_3 \tag{47}$$

Equation (41) may be refined further by replacing the time rate-of-change in C_1 with expressions that are functions of the transported variables U, V and W. From the chemical-relation equation (33), it follows that

$$\frac{\partial}{\partial t}(K_{13}C_1\bar{C}_3) = \frac{\partial}{\partial t}(\bar{C}_1C_3)$$

Rearranging and applying the product rule of differentiation yields:

$$K_{13}C_1\frac{\partial\bar{C}_3}{\partial t} + K_{13}\bar{C}_3\frac{\partial C_1}{\partial t} - \bar{C}_1\frac{\partial C_3}{\partial t} - C_3\frac{\partial\bar{C}_1}{\partial t} = 0 \tag{48}$$

The number of derivatives is reduced by using equation (39) and rewriting $\frac{\partial\bar{C}_3}{\partial t}$ in terms of $\frac{\partial\bar{C}_1}{\partial t}$. This enables common coefficients to be combined such that equation (48) becomes

$$(K_{13}C_1 + C_3)\frac{\partial\bar{C}_1}{\partial t} = K_{13}\bar{C}_3\frac{\partial C_1}{\partial t} - \bar{C}_1\frac{\partial C_3}{\partial t} \tag{49}$$

or

$$\frac{\partial\bar{C}_1}{\partial t} = \frac{1}{g}\left[f_1\frac{\partial C_1}{\partial t} - f_2\frac{\partial C_3}{\partial t}\right] \tag{50}$$

where

$$g = K_{13}C_1 + C_3$$

$$f_1 = K_{13}\bar{C}_3$$

$$f_2 = \bar{C}_1$$

To be of use, however, these coefficients need to be expressed in terms of known or explicitly solvable variables. Accordingly, equation (47) together with (33) and (35) are used to replace C_3, $\bar{C}_3$ and $\bar{C}_1$, such that

$$g = K_{13}C_1 + V - W \tag{51}$$

$$f_2 = (K_{13}C_1\bar{C}_T)/g \tag{52}$$

$$f_1 = K_{13}(\bar{C}_T - f_2) \tag{53}$$

The final step is to rewrite the aqueous concentration derivatives in equation (50). The derivative of C_3 is easily converted: from equation (47), it follows that

$$\frac{\partial C_3}{\partial t} = \frac{\partial V}{\partial t} - \frac{\partial W}{\partial t} \tag{54}$$

The conversion of $\frac{\partial C_1}{\partial t}$ is slightly more involved. An explicit relationship for C_1 in terms of the combined variables U and W must first be developed prior to determining the differential. By combining equations (34) and (44), C_1 may be defined as

$$C_1 = \frac{W}{(1+K_{12}C_2)} \tag{55}$$

Similarly, using equations (34) and (45),

$$C_2 = \frac{U}{(1+K_{12}C_1)} \tag{56}$$

Equation (56) can now be introduced into equation (55) for C_2, and the result expanded into the following quadratic equation,

$$K_{12}C_1^2 + (1 + K_{12}U - K_{12}W)C_1 - W = 0 \tag{57}$$

which may be solved directly for C_1. Applying the quadratic formula yields:

$$C_1 = \tfrac{1}{2}[W - U - (1/K_{12})] + \tfrac{1}{2}\{[W - U - (1/K_{12})]^2 + 4(1/K_{12})W]\}^{\frac{1}{2}}$$

$$= \tfrac{1}{2}A + \tfrac{1}{2}B$$

$$= \tfrac{1}{2}(A + B)$$

where

$$A = W - U - (1/K_{12})$$

$$B = [A^2 + 4(1/K_{12})W]^{\frac{1}{2}}$$

The time derivative of C_1 required for equation (50) is best obtained from the quadratic equation. Accordingly, differentiating (57) with respect to time yields:

$$2C_1 \frac{\partial C_1}{\partial t} + [(1/K_{12}) + U - W] \frac{\partial C_1}{\partial t} + C_1\left(\frac{\partial U}{\partial t} - \frac{\partial W}{\partial t}\right) - (1/K_{12})\frac{\partial W}{\partial t} = 0$$

or

$$[2C_1 + (1/K_{12}) + U - W] \frac{\partial C_1}{\partial t} = [(1/K_{12}) + C_1] \frac{\partial W}{\partial t} - C_1 \frac{\partial U}{\partial t}$$

This can be simplified in terms of B as

$$B \frac{\partial C_1}{\partial t} = [(1/K_{12} + C_1] \frac{\partial W}{\partial t} - C_1 \frac{\partial U}{\partial t}$$

which implies

$$\frac{\partial C_1}{\partial t} = \frac{1}{B} [(1/K_{12}) + C_1] \frac{\partial W}{\partial t} - \frac{C_1}{B} \frac{\partial U}{\partial t} \qquad (58)$$

By substituting equations (54) and (58) for $\frac{\partial C_3}{\partial t}$ and $\frac{\partial C_1}{\partial t}$ respectively, it is possible to rewrite equation (50) as

$$\frac{\partial \bar{C}_1}{\partial t} = \left(\frac{f_1}{g}\right)\left[\left(\frac{(1/K_{12}) + C_1}{B}\right) \frac{\partial W}{\partial t} - \frac{C_1}{B} \frac{\partial U}{\partial t}\right] - \left(\frac{f_2}{g}\right)\left(\frac{\partial V}{\partial t} - \frac{\partial W}{\partial t}\right)$$

$$= \left(\frac{1}{g}\right)\left\{\frac{f_1[(1/K_{12}) + C_1]}{B} + f_2\right\} \frac{\partial W}{\partial t} - \left(\frac{f_1}{g} \frac{C_1}{B}\right)\frac{\partial U}{\partial t} - \left(\frac{f_2}{g}\right)\frac{\partial V}{\partial t}$$

This latter expression may, in turn, be substituted into equation (41), and rearranged to read:

$$\left\{\varepsilon + \rho_b(1/g)\left[f_2 + \frac{f_1[(1/K_{12}) + C_1]}{B}\right]\right\} \frac{\partial W}{\partial t} =$$

$$L(W) + Q(W^* - W) + \rho_b(1/g)\left[\left(\frac{f_1 C_1}{B}\right) \frac{\partial U}{\partial t} + f_2 \frac{\partial V}{\partial t}\right] \qquad (59)$$

Equation (59) together with equations (42) and (43) comprise the basic set of transport equations solved by SATRA-CHEM when binary ion exchange simultaneously occurs with an aqueous equilibrium reaction. Note equation (59) is in the same form as both equations (7) and (30). In this case, the coefficients k_1 and k_2 are defined as

$$k_1 = (1/g)\left[f_2 + \frac{f_1[(1/K_{12}) + C_1]}{B}\right] \qquad (60)$$

$$k_2 = (1/g)\left[\left(\frac{f_1 C_1}{B}\right)\frac{\partial U}{\partial t} + f_2 \frac{\partial V}{\partial t}\right] \qquad (61)$$

When binary ion exchange occurs without an accompanying aqueous reaction, the derivation just described must be adjusted to allow K_{12} to equal zero. Currently, k_1 approaches infinity when $K_{12} = 0$ (equation 60). In chemical systems defined only by R4, $W = C_1$ (equation 44); therefore, the quadratic equation (57) is not required, and the variables A and B, both of which contain the term $(1/K_{12})$, are not defined Moreover, it follows that

$$\frac{\partial W}{\partial t} = \frac{\partial C_1}{\partial t}$$

thus equation (58) is similarly omitted. Consequently, when $K_{12} = 0$, equation (59) becomes

$$\left[\varepsilon + \frac{\rho_b}{g}(f_1 + f_2)\right]\frac{\partial W}{\partial t} = L(W) + Q(W^* - W) + \left(\frac{\rho_b f_2}{g}\right)\frac{\partial V}{\partial t}$$

and the coefficients of equations (60) and (61) are redefined as

$$k_1 = (1/g)[f_1 + f_2]$$

$$k_2 = (1/g) f_2 \frac{\partial V}{\partial t}$$

Overview of Solution Algorithm

Although the coefficients k_1 and k_2 appear complex, the solution procedure for each dependent variable in the transport equations is very similar to that followed in the previous case of equilibrium sorption. The model first solves the linear transport equations (42) and (43) at

t^k for U and V respectively. Equation (59), which is nonlinear, is then solved for W using an iterative process. The first step in this process is to determine systematically all variables represented by k_1 and k_2. This is done through calculations that take advantage of the explicit expressions, defined previously, when solved in the following order:

1. $A = W - U - (1/K_{12})$
2. $B = [A + 4(1/K_{12})W]^{\frac{1}{2}}$
3. $C_1 = \frac{1}{2}(A+B)$
4. $g = K_{13}C_1 + V - W$
5. $f_2 = (K_{13}C_1\bar{C}_T)/g$
6. $f_1 = K_{13}(\bar{C}_T - f_2)$

In these calculations values of W represent the previous iteration, or The previous time step if on the first iteration. With K_{12}, K_{13}, and $\bar{C}_T$ known from the input data, equations (60) and (61) can be solved for k_1 and k_2, and equation (59) is then in a position to be solved for W. If the difference between values of W for successive iterations is greater than a specified tolerance at any node, new values of k_1 and k_2 are determined and the solution process for W is repeated. If the difference is less than the tolerance, the model proceeds to the next time step.

Once W has converged, the concentrations C_2 and C_3 are back-calculated from equations (45) and (47). Note this solution procedure does not require Newton-Raphson iterations for the calculation of C_1 because it can be determined directly from the quadratic equation (57) and the variables A and B.

REQUIRED INPUT DATA

Inasmuch as the model must first solve the hydraulic head at each node, data necessary to solve the ground-water flow equation must be supplied. This includes the components of hydraulic conductivity tensor for each element (i.e., the principal conductivities, together with the angle relating the principal directions to the actual coordinate system) as well as the appropriate initial and boundary conditions as they pertain to the head solution. Additionally, for transient flow, specific storage data are required on a nodewise basis.

The basic transport solution requires the input of longitudinal and transverse dispersivities for each element, and porosity values for each node. Moreover, prior to the simulation of either chemical system, up to four additional parameters are needed depending on the number of reactions involved. These parameters include: (1) either F, the linear sorption coefficient or $\bar{C}_T$, the exchange capacity of the media; (2) K_{12}, the equilibrium constant for reaction R2 (or R5); (3) either K_{13}, the selectivity coefficient for reaction R4 or K_{14}, the equilibrium constant for reaction R3; and (4), the solid-grain density.

The parameter F is commonly determined for specific soils through laboratory analysis, and is primarily a function of minerology, particle size, temperature, soil moisture, pH, and Eh (Fetter, 1980). Equilibrium constants are principally a function of temperature, and values for specific reactions may be found in selected chemical

handbooks (e.g. Weast et al., 1983). For further information, a complete listing of the input data requirements for SATRA-CHEM may be found in Appendix B.

NUMERICAL METHODOLOGY

The numerical technique used in the original transport model SATRA remains unchanged in the present version of SATRA-CHEM. Equations (30) and (59) can be solved for flow regimes positioned either areally or in cross section using a mesh comprised of quadralateral finite elements.

SATRA-CHEM employs a Galerkin scheme for spatial approximations of the dependent variable that involves symmetric, and in the case of the advection term, asymmetric basis functions when upstream weighting is employed as an option. These approximations take the form

$$\psi(x,y,t) \approx \hat{\psi}(x,y,t) = \sum_{j=1}^{N} \psi_j(t)\phi_j(x,y)$$

where, ψ represents the dependent variable, N is the number of nodes in the mesh, and ϕ_j is the spatial basis function for node j. Following Galerkin orthogonalization, the resulting integral equations are evaluated in local coordinates using two-by-two Gaussian quadrature.

A matrix equation is assembled in which the advective-dispersive expressions in the form of equation (7) reduce to

$$\underline{\lambda}\psi + \underline{\beta}\psi + \underline{\chi}\frac{\partial \psi}{\partial t} = \underline{\omega}$$

where, $\underline{\lambda}$ is a symmetric coefficient matrix containing the dispersive components, $\underline{\beta}$ is a coefficient matrix (symmetric in the case of no

upstream weighting) that contains the advective contributions, $\underline{\chi}$ is the coefficient matrix for the time derivative containing the nonlinear terms in k_1 (equations (30) and (60)), and $\underline{\omega}$ is the vector of nodal source contributions including the nonlinear terms in k_2 (equations (30) and (61)). A "lumped-mass" approach is used that allows the coefficients in $\underline{\chi}$ to be loaded directly onto the main diagonal. The time derivative is discretized through a backwards finite-difference scheme that yields a fully implicit equation in which the matrix is symmetric (in the case of no upstream weighting) and banded.

The upstream weighting option in SATRA-CHEM is available for stabilizing oscillations in the solution due to highly advective transport. This option, however, only results in an increase in the local longitudinal dispersivity by an amount proportional to the distance between successive nodes along the direction of flow. This weighting factor, therefore, was not used in simulations run for this study, and thus only symmetric basis functions were employed.

The model allows for hydraulic conductivities to be anisotropic and variable in both direction and magnitude on an elementwise basis throughout the system. Boundary conditions as well as all sinks and sources are permitted to vary with time.

The current version of the code uses a direct Gaussian solver for banded matricies which, while highly accurate, remains inefficient in terms of time and storage requirements for very large problems. The incorporation of a more efficient solver is planned for future versions of the model. More detailed information on the specifics of the

numerical method applied in both SATRA and SATRA-CHEM, as well as other program features, may be found in Voss (n.d.).

The computer code is compiled in FORTRAN 77 and has been successfully run on a Prime series 850 computer maintained by the U.S. Geological Survey in Reston, Virginia.

MODEL TESTING AND APPLICATION

The results of several examples are presented to demonstrate the ability of the model to simulate the effects of chemical interaction among transported solutes. Additionally, where possible, analytical solutions are shown to verify that modifications of the original code, SATRA, have not been deleterious to the correctness of the basic transport algorithm. Both the accuracy and precision of the numerical solution generated by SATRA have been successfully tested previously in Voss (n.d.).

Equilibrium Sorption and Aqueous Reactions

The six examples that follow concern the chemical environment characterized by reactions R1 through R3. All simulations involve steady-state flow and a physical system with dimensions typical of field rather than laboratory conditions. Although the model is two dimensional, important trends in the results are best shown in one dimension; therefore, most examples are presented in this perspective. In these cases, the region modeled may be viewed as a representative stream tube within a larger physical setting. Except where noted, the system is defined by the parameters listed in Table 1, and is based on the finite-element mesh shown in Figure 1. All chemical parameters are in an arbitrary system of consistent units, and are specified separately for each example.

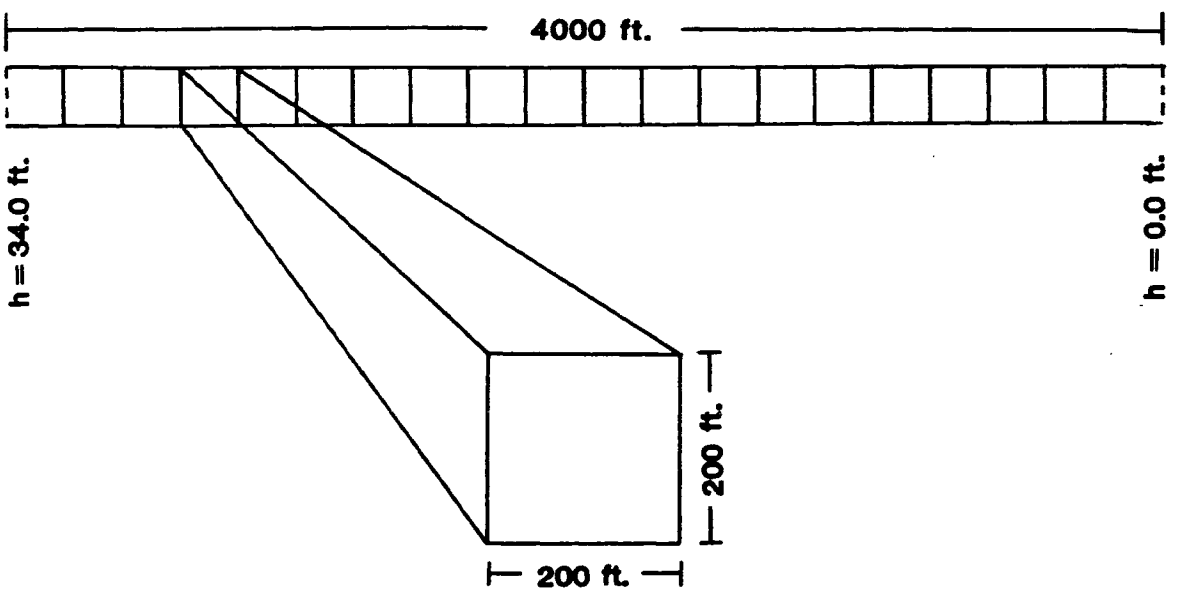

Figure 1. Finite-element mesh and boundary conditions for one-dimensional simulations

Initially, the porous medium is saturated with fluid containing zero concentration of all tenads, i.e., for a system 4000 feet in length (Figure 1):

t=0	0≤x≤4000	C_1=0.0	C_2=0.0	C_4=0.0
		U=0.0	V=0.0	W=0.0

Table 1. Physical Parameters Employed in Model Runs

Porosity (ε)	0.20	
Hydraulic Conductivity ($\underline{K}$)	3.00×10^{-4}	ft/sec
Longitudinal dispersivity (α_L)	100.0	ft
Hydraulic gradient ($\underline{\nabla}h$)	0.0085	
Average pore velocity ($\underline{v}=(K/\varepsilon)\underline{\nabla}h$)	1.28×10^{-5}	ft/sec
Peclet number ($Pe=\Delta x/\alpha_L$)	2.0	

The boundaries are defined by constant heads, h, at both ends of the system:

t≥0	x=0	h=34.0 ft.
t≥0	x=4000	h= 0.0 ft.

The simulation commences as fluid flows continuously into the system across the upstream constant head boundary; upon reaching the downstream Dirichlet boundary, the flow is free to exit the system unimpeded. The inflow solution contains constant concentrations (≥0) of the three tenads alone, or with additional nonreactive ions, in combinations such that an electrostatic balance is maintained. Note an electrostatic balance is a constraint imposed by natural chemical

systems and is independent of the mathematical theory employed by the model. Where arbitrary reactions and concentrations are used in this study for demonstration, a charge balance has been set by the user. Under field conditions, however, chemical analyses of the source fluid should yield the appropriate balance of anion and cation concentrations automatically.

Another important condition that applies to the source fluid is continuous chemical equilibrium among the various components. Aqueous reactions such as R2 and R3 occur in the source fluid if the appropriate components are present and the equilibrium constant is some positive finite value.

The time step interval (Δt) in all one-dimensional examples is selected such that a particle of fluid will progress approximately one element (200 feet) per time step. This interval is the maximum recommended, based on the Courant-Friedrichs-Lewy condition, for stability and convergence in (Eulerian) numerical schemes where nodes are fixed in space (Smith, 1978).

Linear Sorption Alone

Single species adsorption has been addressed extensively in the literature (e.g., Lai and Jurinak, 1972; Pickens and Lennox, 1976; Bear, 1979). The well known net effect of this process is to reduce the average pore velocity of the sorbing solute. The amount of this reduction is a function of the porosity, grain density and sorption coefficient, F. To demonstrate the effect of linear sorption on the average velocity of a line of constant concentration, equation (7) can be

rewritten in terms of a material derivative for concentration C as

$$\frac{DC}{Dt} = \left(\frac{1}{\varepsilon + (1-\varepsilon)\rho_s k_1} \right) [\underline{\nabla}\cdot(\varepsilon \underline{\underline{D}}\cdot\underline{\nabla}C) + Q(C^* - C) - (1-\varepsilon)\rho_s k_2]$$

$$= \frac{\partial C}{\partial t} + \underline{v}\cdot\underline{\nabla}C$$

$$= \frac{\partial C}{\partial t} + \Phi\underline{v}\cdot\underline{\nabla}C$$

where

$$\Phi = \left(\frac{\varepsilon}{\varepsilon + (1-\varepsilon)\rho_s k_1} \right) = R^{-1}$$

The term R represents the reduction in the average fluid velocity caused by sorption, and is equivalent to the retardation factors discussed by Lai and Jurinak (1972), and van Genuchten and Alves (1982) among others. In this case, without additional aqueous reactions, the calculation of R is straight forward because $k_1 = F$. This follows from equation (28) which sets $H = 1.0$ when $K_{12} = K_{14} = 0.0$.

Figure 2 shows the effect of linear sorption on M_1 without any accompanying homogeneous reactions after 14 time steps (approximately 7 years). The inflowing solution contains concentrations of 1.0 for C_1, C_2 and C_4.

Using the parameters in Table 1 and a value of 0.1 for F, a Φ equal to 0.33 can be calculated. This implies that the C_1 front should travel at an average velocity that is roughly a third as fast as the conservative (non-sorbed) concentrations C_2 and C_4. In terms of the figure, the 50 percent relative concentration of the conservative solutes should travel a distance of 2800 feet or 14 elements; the same level of the sorbed solute should travel a distance of 930 feet, or

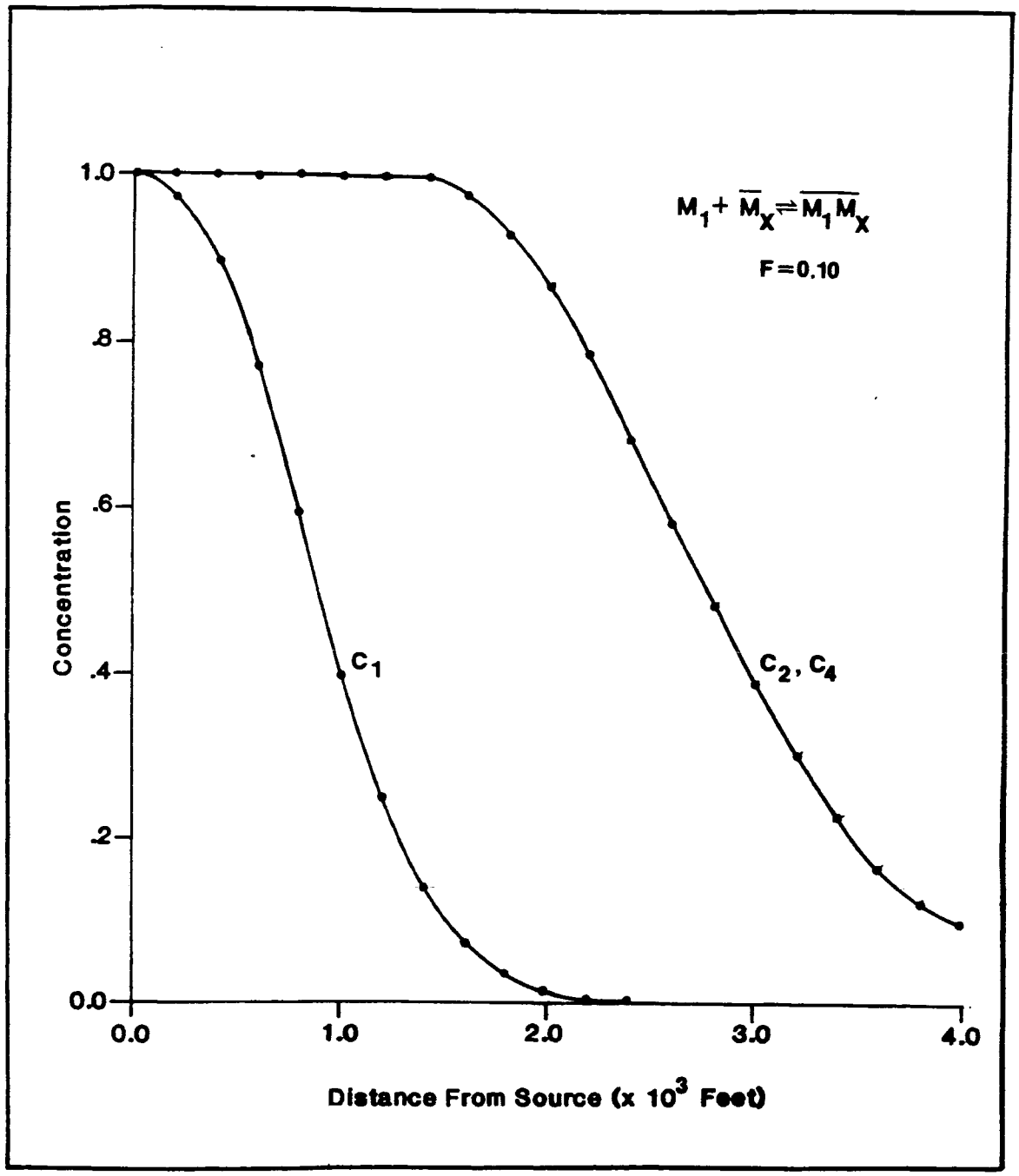

Figure 2. Single species sorption (R1, F = 0.1) and conservative transport (C_2, C_4) after 14 time steps (approximately 7 years)

slightly past midway into the fifth element. The results produced by the model come close to these values (within 2 percent).

The exact solution for the entire distribution of both the sorbed and conservative fronts can be determined by recognizing that this problem may be described by rewriting equation (7) in one dimension to read

$$R \frac{\partial U}{\partial t} = D_x \frac{\partial^2 U}{\partial x^2} - v_x \frac{\partial U}{\partial x} \qquad \text{on } 0 \leq x \leq L = 4000$$

subject to:

$$U(x,0) = 0$$

$$D_x \frac{\partial U}{\partial x} + v_x U|_{x=0} = v_x U_0 \qquad (U_0 = 1.0) \quad t > 0$$

$$\frac{\partial U}{\partial t}(L,t) = \text{finite}$$

The analytical solution, as reported by van Genuchten and Alves (1982), is

$$U(x,t) = \tfrac{1}{2} \operatorname{erfc}\left[\frac{Rx - vt}{2(DRt)^{\frac{1}{2}}}\right] + \left(\frac{v^2 t}{\pi DR}\right)^{\frac{1}{2}} \exp\left[-\frac{(Rx - vt)^2}{4DRt}\right]$$

$$- \frac{1}{2}\left(1 + \frac{vx}{D} + \frac{v^2 t}{DR}\right) \exp(vx/D) \operatorname{erfc}\left[\frac{Rx + vt}{2(DRt)^{\frac{1}{2}}}\right] \qquad (62)$$

where R = 1.0 for conservative transport. Figure 3 contains the analytical solutions for both fronts plotted as solid lines, and the corresponding model results represented by points. Although errors in the results produced by the model are enhanced at the scale used in

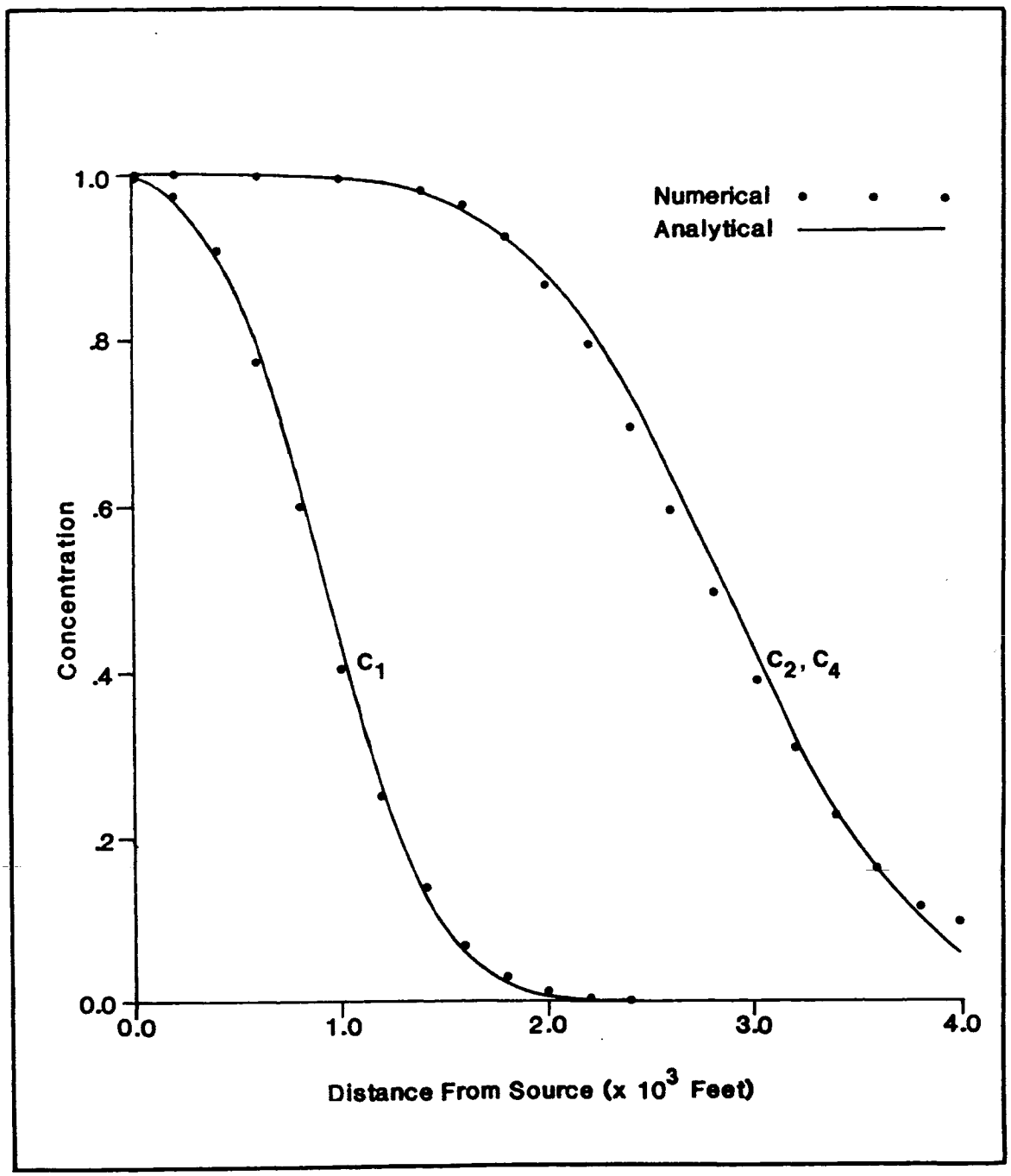

Figure 3. Numerical versus analytical solutions for single species sorption (R1, F = 0.01) and a conservative transport (C_2, C_4) after 14 time steps

Figure 3, the results agree well with the exact solutions for both the conservative and sorbed distributions. Any deviation from the analytical solution may be reduced by decreasing the nodal spacing and/or the time step increment.

Aqueous Equilibrium Reactions Alone

The concentration distributions of transported solutes participating in aqueous equilibrium-controlled reactions are shown after eight time steps (approximately 4 years) in Figures 4 and 5. Figure 4 represents a chemical system defined only by reaction R2 with an inflow concentration of 1.0 for C_1, C_2 and C_4. The input of C_4 allows the distribution of a conservative solute to be illustrated simultaneously with reacting solutes.

Figure 4 shows an important trend that is unique to equilibrium-controlled reactive transport: the concentration front for the reactive species (C_1 and C_2) has higher values downstream than that of the conservative equivalent (C_4). Conceptually, a reactive species has these higher concentrations because at every point in the system it is in equilibrium with a dissolved compound that contains additional amounts of that species. Along the solute front, reduction in the concentration of the reactants causes R2 to proceed to the left creating more of these reaction participants through dissociation. Without the reactive capability, a species lacks this additional 'source' and its concentration drops off more rapidly.

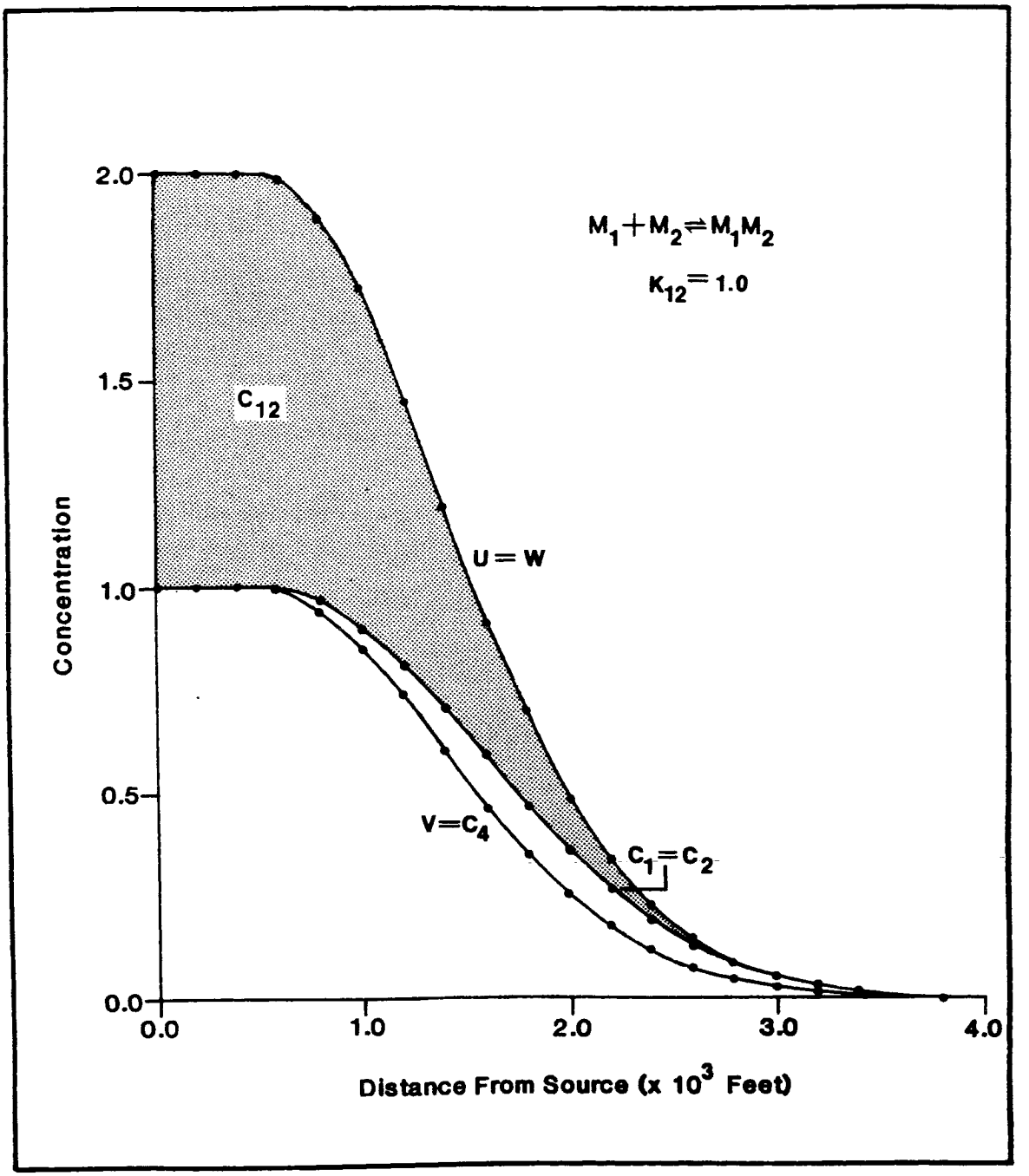

Figure 4. Transport with one aqueous equilibrium reaction (R2, K_{12} = 1.0) and a conservative solute (C_4) after 8 time steps (approximately 8 years)

Mathematically, this situation arises because the actual transported quantities, in terms of the model, are the total dissolved tenad concentrations U, V and W. These distributions are also plotted in the figure. When M_1 reacts with M_2 the concentration of the dissolved species C_{12} is added to both U and W (equations (13) and (15)); but, without reaction R4, no C_{14} is available to add to V. Consequently, U and W are greater than V at every point in the system even though they are all governed by the same initial and boundary conditions. All three solutes (U, V and W) represent conservative quantities because no sorption is involved, and the total masses of $\{M_1\}$, $\{M_2\}$ and $\{M_4\}$ are reaction-independent. The individual concentrations C_1 and C_2, however, are a function of the reaction, and thus are not transported conservatively. These latter concentrations are determined through equation (32) which reduces to a quadratic when $K_{14} = 0$. This nonlinear relationship produces values of C_1 and C_2 that are constantly in equilibrium with C_{12} (shaded are in the figure) given the distributions of U and W.

Inasmuch as the distributions of U, V and W are conservative, their values can be verified through the same analytical solution (62) that was applied in the previous section. Additionally, while the entire concentration front of $C_1 = C_2$ cannot be checked against an exact solution, specific points along the front may be verified provided values of U or W are known. The following brief calculation demonstrates this idea, and serves as a check that the model is obtaining concentrations at equilibrium.

The 50 percent level of concentration for U (or W) is equal to 1.0, and it should coincide at the same point in space with the 50 percent level of V (or C_4) which is equal to 0.5. The amount of C_1 at the same point can be calculated using the cubic equation (32) which reduces to the following quadratic when R2 is the only reaction:

$$K_{12}C_1^2 + [1 + K_{12}(W-U)]C_1 - W = 0$$

In this case, $K_{12} = 1.0$, and $W = U = 1.0$; as a result, the quadratic becomes

$$C_1^2 + C_1 - 1 = 0$$

Applying the quadratic formula yields only one positive root namely, $C_1 = 0.620$. The model should produce this same value of C_1 at the point where the conservative distributions are at 50 percent relative concentration. A check with Figure 4 indicates the model is correct.

Figure 5 shows the concentration distributions for a chemical transport system defined by both reactions R2 and R3. The inflow concentrations of C_2 and C_4 are set at 1.0, while C_1 is input at twice this level to maintain an electrostatic balance. The equilibrium constants are $K_{12} = 0.5$ and $K_{14} = 5.0$.

The figure shows another important trend resulting from the transport of equilibrium-controlled solutes: the participants in the reaction with the higher equilibrium constant has higher values downstream. This result follows from the previous discussion of Figure 4. The higher the equilibrium constant, the the greater the corresponding concentration of C_{ij} for the equivalent input levels of C_i and C_j in both reactions. In this case, the equilibrium conditions imply that C_{14}

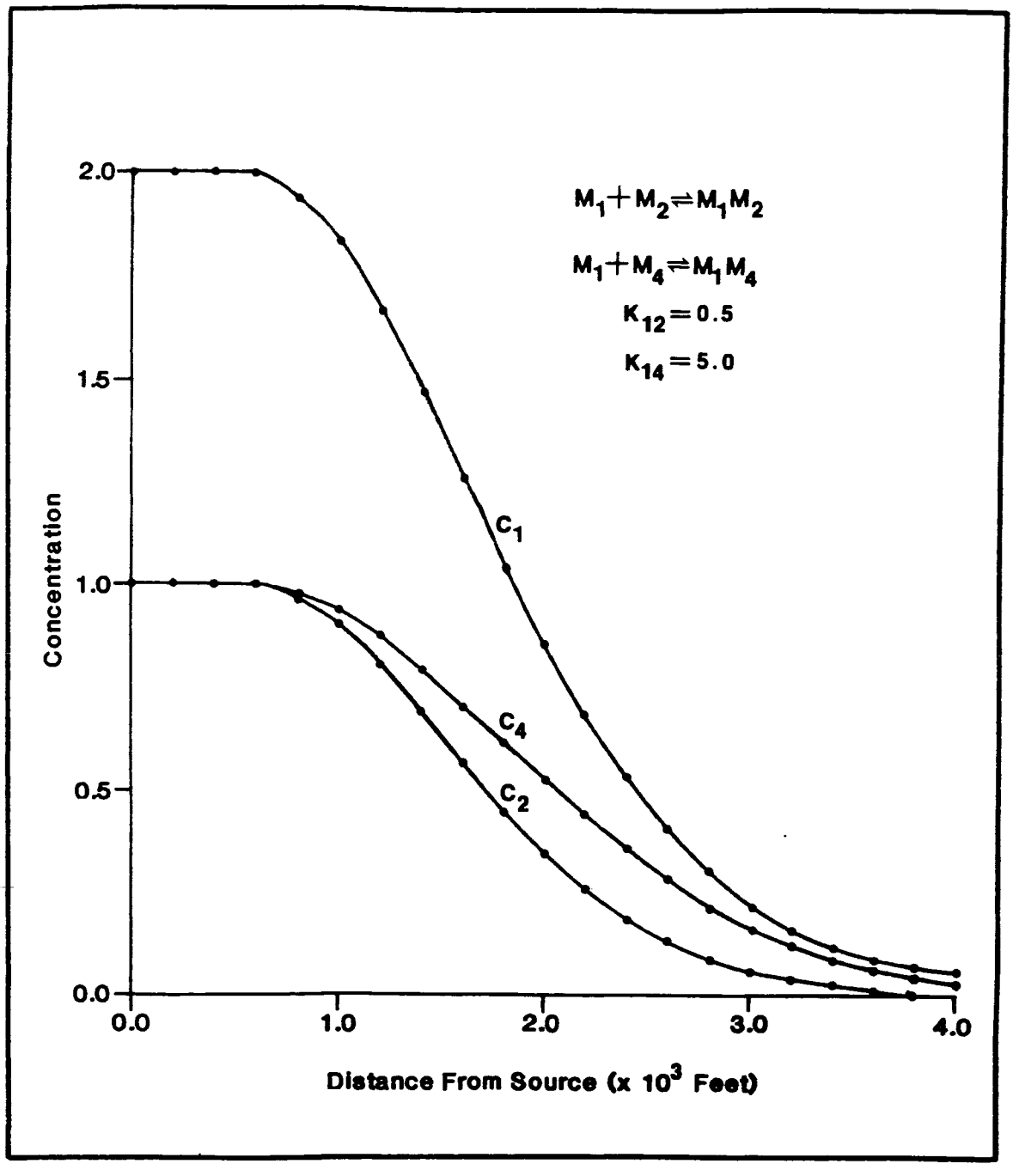

Figure 5. Transport with two simultaneous aqueous equilibrium reactions (R2, K_{12} = 0.5 and R3, K_{14} = 5.0) after 8 time steps

is everywhere greater than, or equal to, C_{12}. As result, more C_4 is produced (relative to C_2) as both reactions proceed to the left along their respective fronts.

The mathematics can be traced to equations (13) and (14), together with (20) and (21), in which a larger K_{14} corresponds with a higher value of V relative to U (for a given C_1). A higher V, in turn, yields values of C_4 that are greater than C_2 when the individual reactant concentrations are back-calculated in equations (22) and (23).

The difference between the resulting distributions of C_2 and C_4 is not, however, directly proportional to the difference in their respective equilibrium constants. The values of these constants dictate the initial levels of U, V and W in the source fluid. But the presence of the equilibrium constants in the denominator of both equations (22) and (23) offsets, to some degree, the effect of a larger total dissolved tenad concentration when the individual reactant concentrations are back-calculated during transport.

Sorption and One Aqueous Reaction

The next example involves the transport of a chemical system in which linear sorption (R1) and an aqueous equilibrium reaction (R2) occur simultaneously. The interrelationships among the two reactions and the equilibrium conditions imposed on the system cause the sorption of M_1 to directly affect the resulting distribution of C_2. The nature of the effect depends on the sorption coefficient, the equilibrium constant and the amount of elapsed time.

Several runs were made to demonstrate the effect of varying the parameters F and K_{12} on this reaction combination. Constant and continuous inflow concentrations of 1.0 for all three reactant species were maintained for each run. The transport of C_4 was included in these simulations to represent a conservative solute for comparison.

Note the results generated by the model for hybrid chemical systems cannot be easily checked because no analytical solutions are available. The accuracy of the results, therefore, will not be proved but is implied based on the verifications presented above. In the following examples a knowledge of the fundamental concepts of equilibrium chemistry and linear sorption are relied upon to explain the various distributions produced by the model when simulating these reactions.

The results for F = 0.25 and K_{12} = 1.0 are shown in Figure 6. The distribution of C_2 is characterized by a rise and fall in concentration that peaks at almost twice the inflow level. These results are best explained by referring to the reactions (R1 and R2). Because the system is at equilibrium, as M_1 is taken out of solution to form $\bar{M}_1$ the reaction R2 is forced to proceed toward the left. This causes M_1M_2 to dissociate producing both M_1 and M_2. With the sorption of M_1, the system maintains equilibrium through the increased amount of M_2 in solution.

The magnitude and extent of the peak level of C_2 are determined by the equilibrium condition that balances R2 according to the degree of sorption in R1, and the transport mechanisms of advection and dispersion. These factors combine to cause the level of C_2 to peak at the

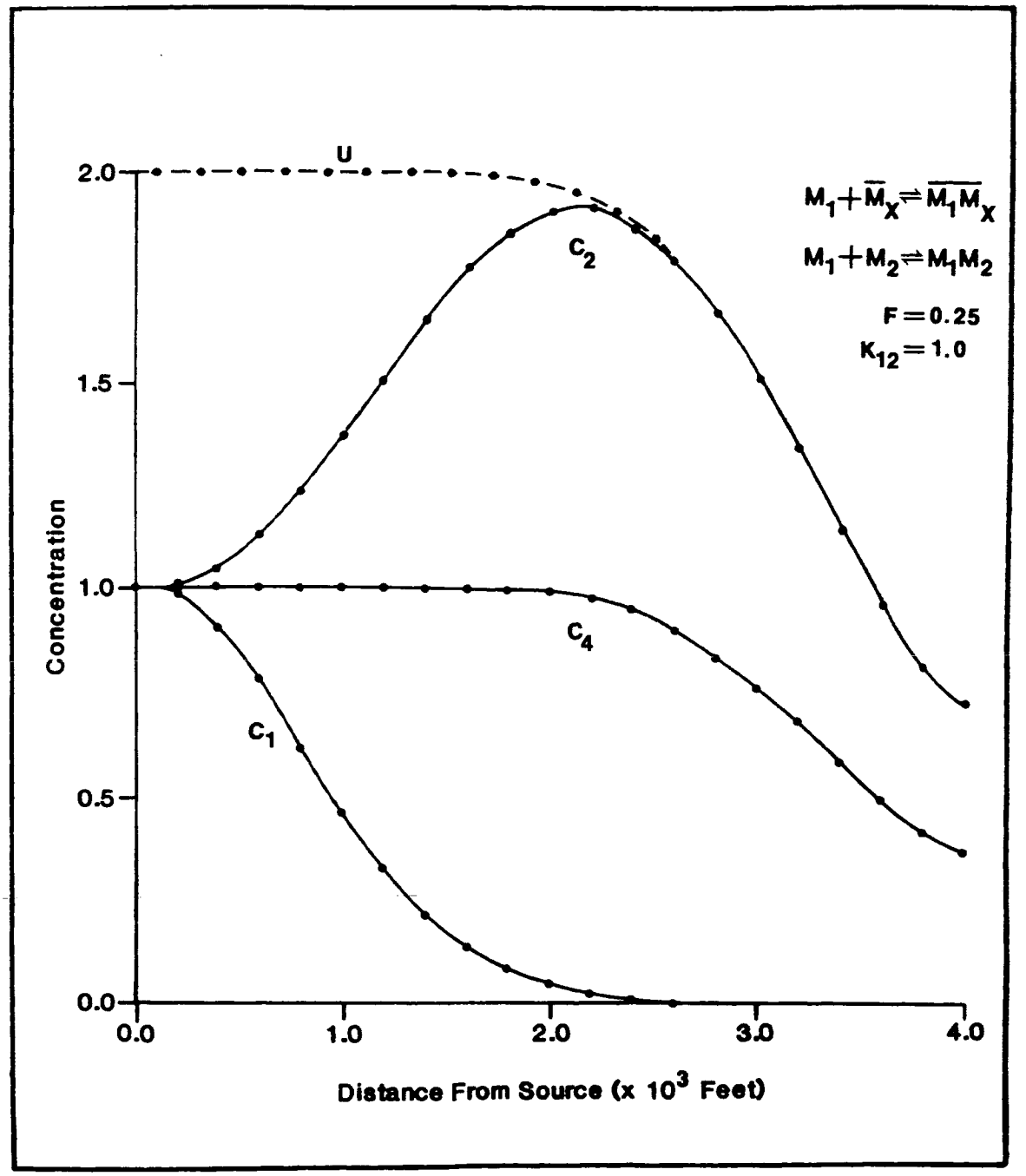

Figure 6. Transport with equilibrium sorption (R1, F = 0.25) and one aqueous complexation (R2, K_{12} = 1.0) after 18 time steps (approximately 9 years)

point of maximum difference between the sorbed (C_1) and the equivalent conservative concentration (C_4). The maximum amount of M_2 produced is limited by the total dissolved $\{M_2\}$ concentration, U, in the source fluid. For reference, the conservative distribution of U is included in both Figures 6 and 7. The concentrations C_2 and U become the same at the point where C_1 equals zero. Past this point, both reactions R1 and R2 stop because M_1 is no longer available to react. If M_1 is highly sorbed, such that C_1 reaches zero at a point where the conservative solute equals its inflow concentration, then C_2 will equal U at the maximum possible level. If M_1 is not highly sorbed, however, then C_2 will equal U at some point along the latter's concentration front.

An increase in either the sorption coefficient F, or the equilibrium constant K_{12}, will increase the peak concentration of M_2 as shown in Figures 7 and 8 respectively. The greater the value of F, for a given K_{12}, the more M_1 is sorbed as illustrated by sharper C_1 profiles in Figure 7. The result is a rapid increase in the production of M_2 near the inflow that reaches the maximum level dictated by the boundary condition on U. When F is relatively low, M_1 is sorbed less and the difference between C_1 and the conservative C_4 is smaller. This allows equilibrium to be maintained through lower levels of C_2. Moreover, with low values of F, the peak in C_2 does not correspond with U because C_1 does not equal zero at the point of maximum difference between the sorbed and equivalent conservative solutes.

Figure 8 shows the effects of progressively larger values of K_{12} (for constant F) on the distribution of C_2. A higher peak is associated

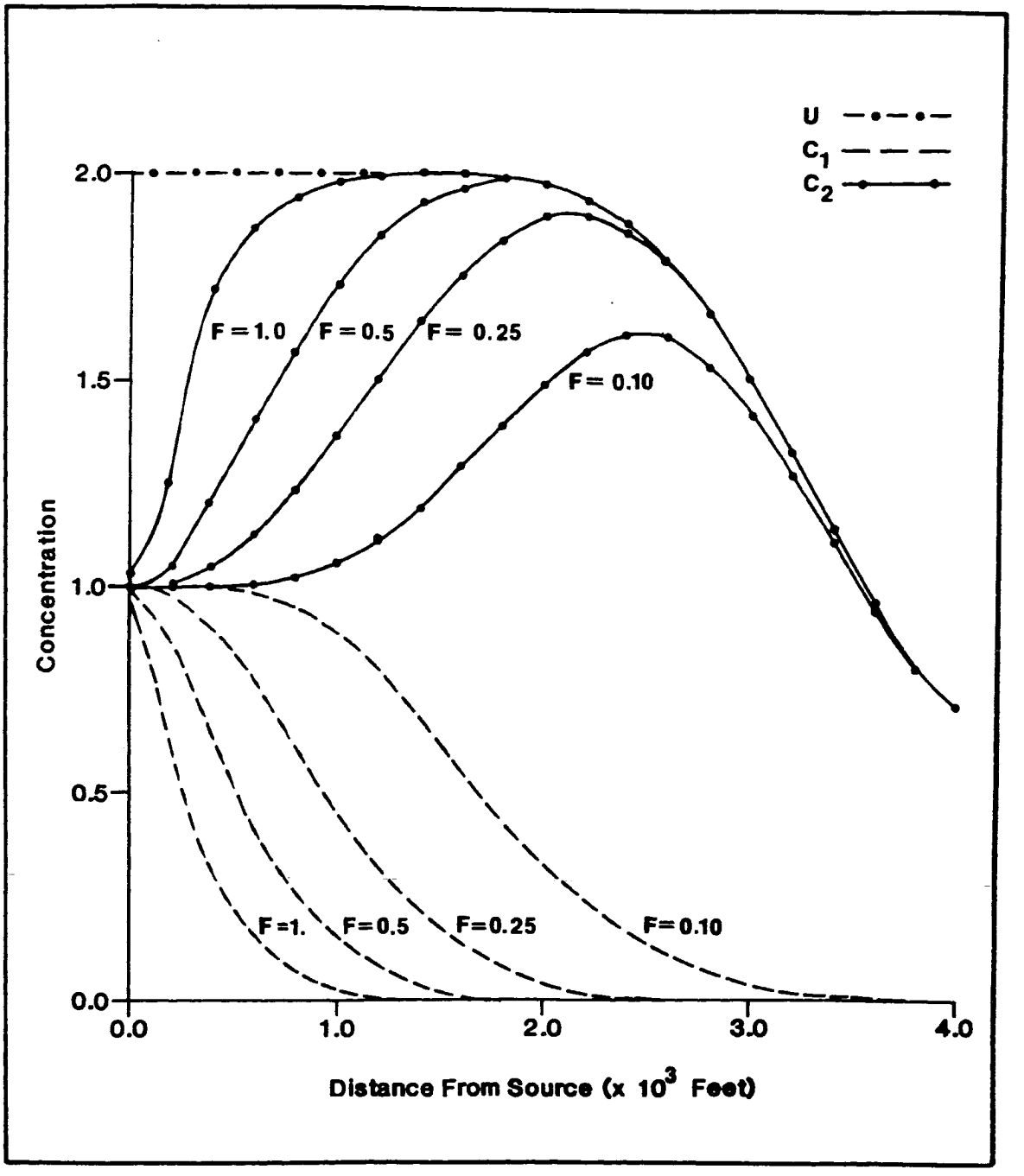

Figure 7. The effect of the sorption coefficient, F, on the distributions of C_1 and C_2 when linear sorption (R1) and an aqueous equilibrium reaction (R2, K_{12} = 1.0) occur together during transport

with a greater K_{12} because the level of C_{12} at equilibrium throughout the system is correspondingly greater. This causes U, in turn, to be greater as well. Moreover, as U is increased, the potential limit on the peak in C_2 is also increased. Additional C_{12} implies that C_1 will have a longer front (not shown) due to the latter's increased inherent presence in both U and W. Consequently, the peak in C_2 is shifted downstream. In addition, the magnitude of the peak is greater because for a given level of M_1 sorbed, more M_2 is required as the equilibrium condition with M_1M_2 is increased.

The peak level of C_2, as dictated by F and K_{12}, will increase with time until it either coincides with U, or until C_1 reaches the outflow. This trend is illustrated in Figure 9 through successive distributions of C_2 for the same chemical parameters used to obtain the results in Figure 6. Although the decline in peak C_2 is not shown, it will occur as soon as $C_1>0$ throughout the system. Past that time, the difference between C_1 and the conservative C_4 gradually decreases until both concentrations are equal (steady-state solution).

Note the steady-state solution for C_2 will show no increase in concentration above its inflow level. At sufficiently late time, C_1 will reach its source concentration level at every point, and the sorption limit (as defined by the boundary condition on C_1) will be attained as well. With no sorption, there is no production of M_2; thus the steady-state solution to this problem is the same as if no reactions or sorption occured.

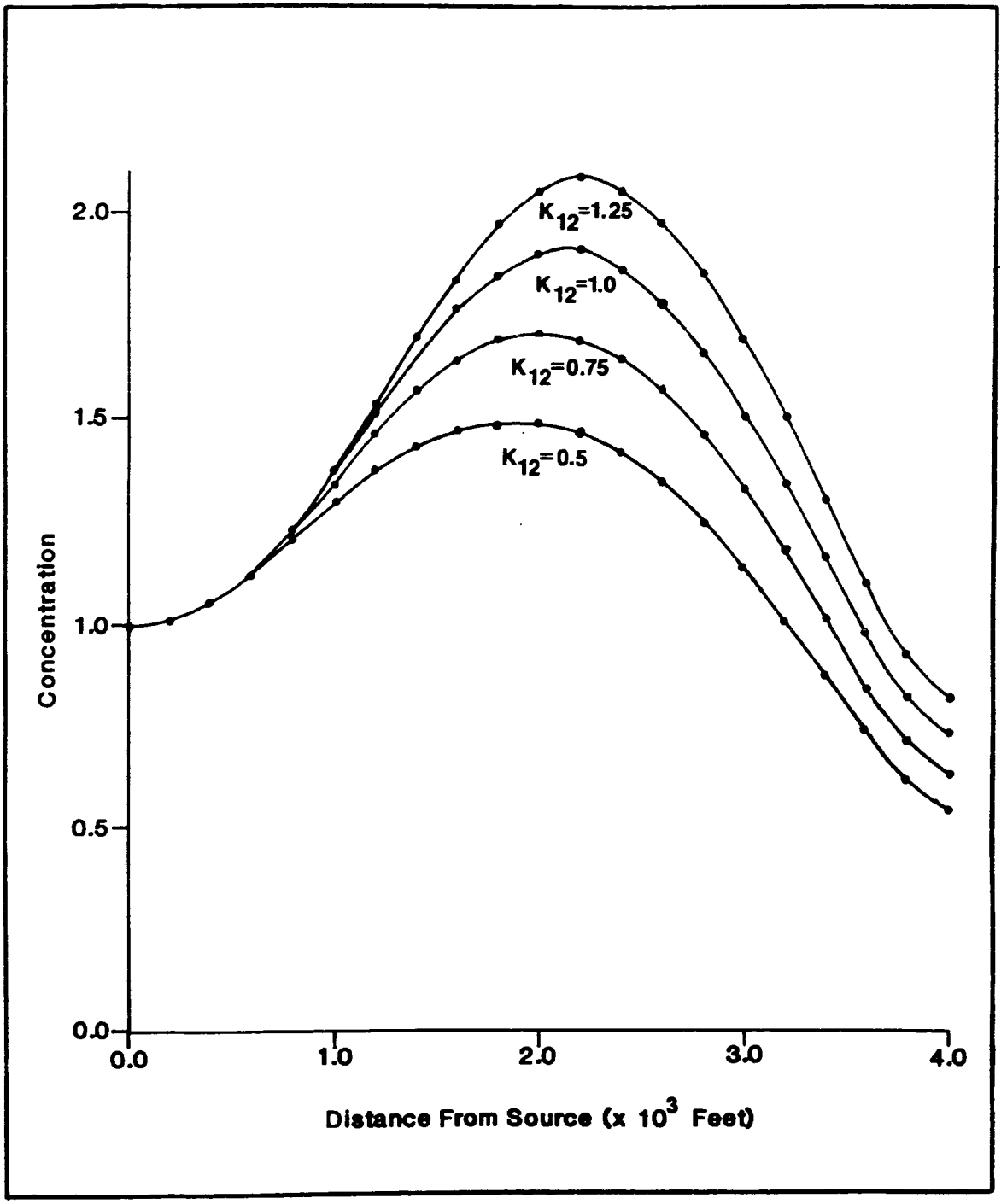

Figure 8. The effect of the equilibrium constant, K_{12}, on the distribution of C_2 when linear sorption (R1, F = 0.25) and an aqueous equilibrium reaction (R2) occur simultaneously during transport

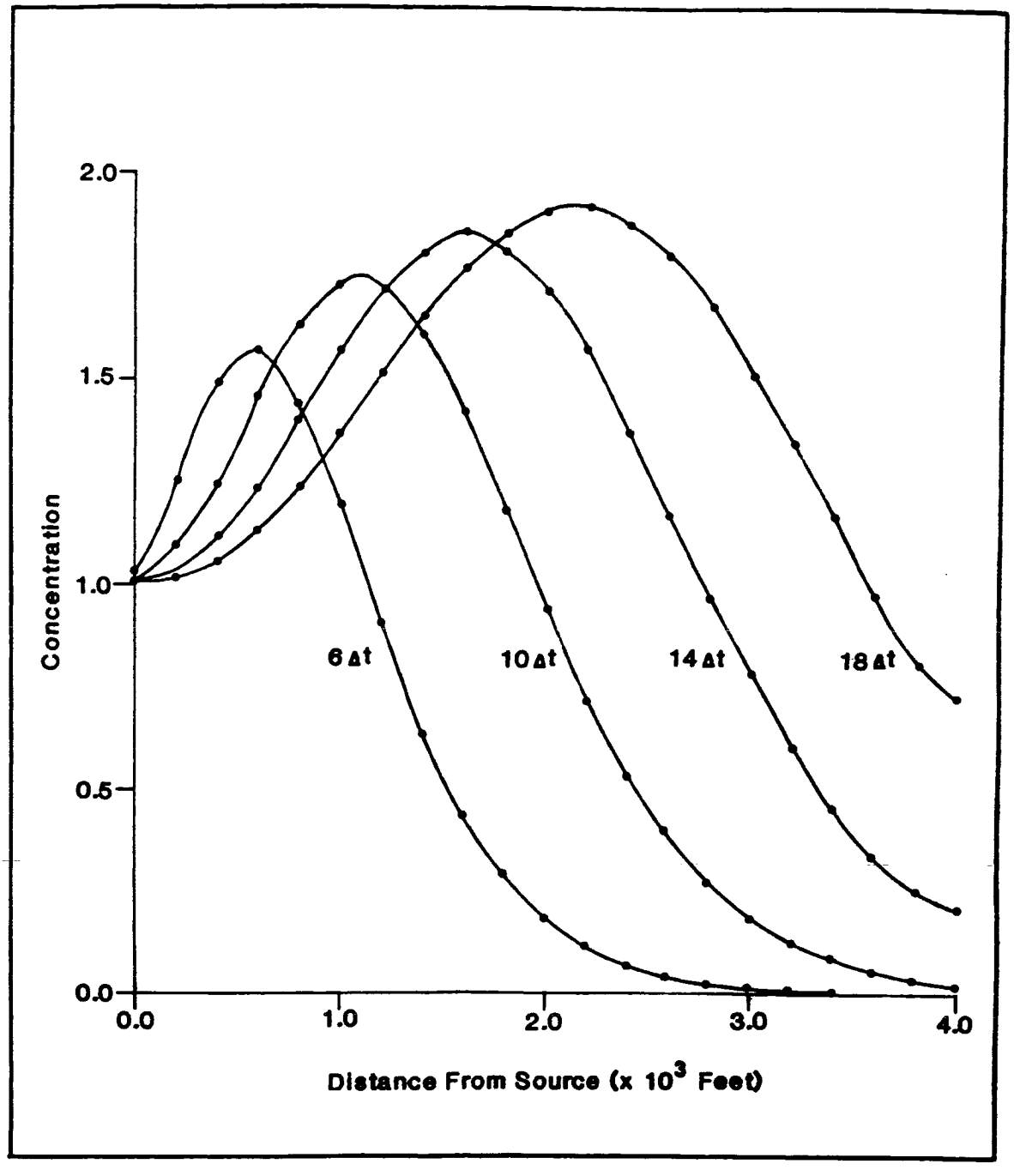

Figure 9. The effect of elapsed time on the distribution of C_2 when linear sorption (R1, F = 0.25) and an aqueous equilibrium reaction (R2, K_{12} = 1.0) occur simultaneously during transport

Sorption and Two Aqueous Reactions

The next example combines all three reactions (R1 through R3) using the following chemical parameters: F = 0.25; K_{12} = 0.5; and K_{14} = 1.0. The inflowing solution contains concentrations of $C_2 = C_4 = 1.0$; and $C_1 = 2.0$.

Figure 10 shows the results produced by the model after 18 time steps. The sorption of M_1 again directly affects the distributions of C_2 and, in this case, C_4 as well. Both concentrations increase above their inflow values, but differ as a function of their respective equilibrium constants. The distribution of C_4 has the higher peak because it is associated with the larger constant. As noted earlier, a higher K_{ij} implies a greater ratio of product to reactant concentrations, and thus more C_{ij} is available for the production of both C_i and C_j. The sorption of M_1 simultaneously decreases C_{12} and C_{14} by equal amounts, but the greater equilibrium constraint imposed on R3 requires C_4 to increase more than C_2.

Sorption and Aqueous Reactions: An Example with Cd, SO_4 and NTA

The trends produced when simulating arbitrary reactions and chemical parameters should also occur when real values are employed. Rubin (1983b) suggested an example involving reactions R1 through R3 in which the chemical system is comprised of the following components:

1. Adsorption:

$$M_1 + \bar{M}_x \rightleftharpoons \overline{M_1 M_x} \qquad \text{(R1A)}$$

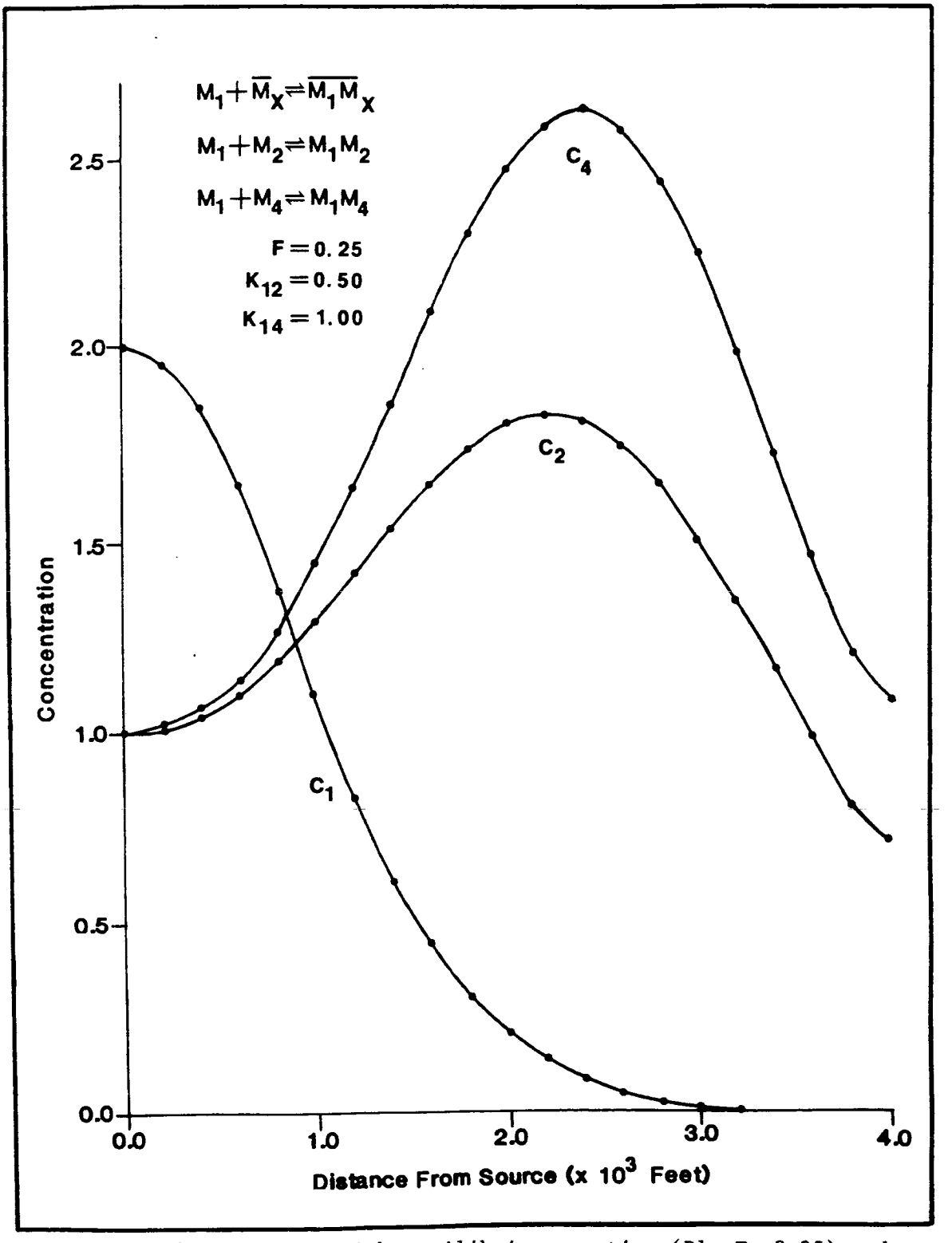

Figure 10. Transport with equilibrium sorption (R1, F =0.25) and two aqueous complexations (R2, K_{12} = 0.5 and R3, K_{14} = 1.0) after 18 time steps

where

$$\{M_1\} = Cd^{2+}$$

$$\{\bar{M}_x\} = \text{porous media}^{2-}$$

2. Inorganic complexation:

$$M_1 + M_2 \rightleftharpoons M_1M_2 \qquad \text{(R2A)}$$

where

$$\{M_2\} = SO_4^{2-}$$

$$M_1M_2 = CdSO_4$$

3. Organic complexation:

$$M_1 + M_4 \rightleftharpoons M_1M_4 \qquad \text{(R3A)}$$

where

$$\{M_4\} = NTA^{3-} \quad \text{(Nitriloacetate)}$$

$$M_1M_4 = (CdNTA)^{-}$$

In addition, a nonreactive tenad $\{M_3\} = Na^{+}$ is present to maintain an electrostatic balance.

Transport containing these reactions was simulated using the model. The simulation was based on a physical system similar to that employed in the runs above; however, the strong tendency for Cd^{2+} to sorb required a reduction in the spatial and temporal dimensions for optimal results. Nodal spacing was reduced by a factor of ten (to 20 feet, 6.1 m) and the time step was decreased such that a particle of fluid would travel a quarter of a element (5 feet, 1.5 m) per time step (i.e., the Courant number was reduced from 1.0 to 0.25). By using the same number of elements (20), the total length of the system decreased to 400 feet (121.9 m). This required the upstream constant head to be

reduced by a similar factor of ten to maintain the same hydraulic gradient and hence fluid velocity. Other values of the physical and chemical parameters used in the simulation of R1A through R3A are listed in Table 2.

Table 2. Physical and Chemical Parameters used in the Simulation of Transport Containing Cd, SO_4 and NTA

Porosity (ε)	0.20
Hydraulic conductivity ($\underline{K}$)	3.00×10^{-4} m/s
Longitudinal dispersivity (α_L)	3.05 m
Sorption coefficient (F)	0.20 m^3/Kg
Equilibrium constant for R2A (K_{12})	6.30×10^{3} m^3/mmole
Equilibrium constant for R3A (K_{14})	2.88×10^{-6} m^3/mmole
Source fluid concentrations:	
Cd^{2+} (C_1)	0.10 mmole/m^3
SO_4^{2-} (C_2)	2000.0 mmole/m^3
NTA^{3-} (C_4)	0.02 mmole/m^3

The results after 56 time steps (approximately 8 months) are shown in Figure 11. Because the reactant concentrations differ by orders of magnitude, close attention should be paid to the appropriate scale. The results then may be interpreted following the discussion of the previous examples.

Although three reactions are involved, R2A plays a relatively minor role because K_{12} is significantly lower than K_{14}. In effect, comparatively little $CdSO_4$ is present; consequently, essentially no

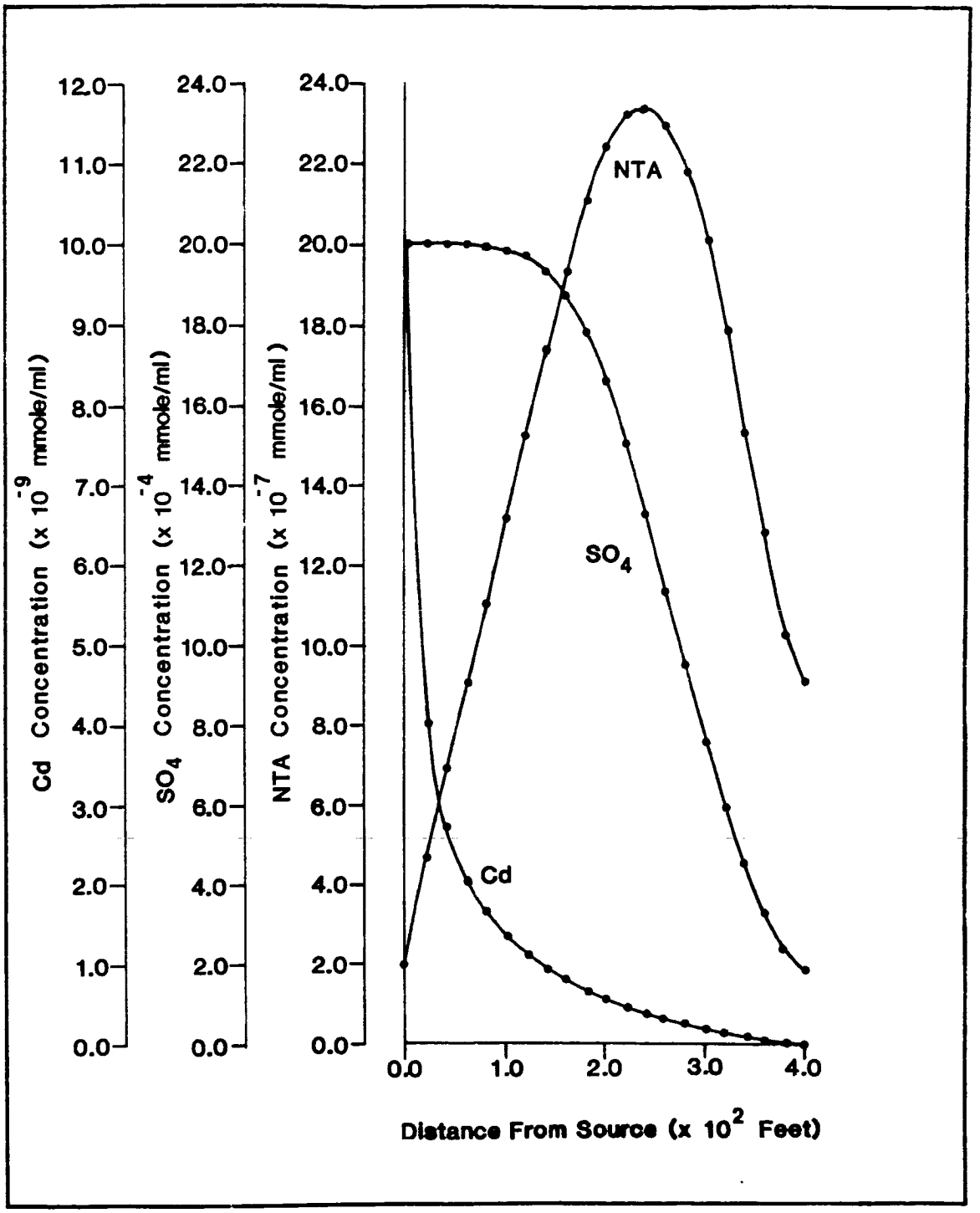

Figure 11. Transport with reactions R1A-R3A involving the sorption of Cd and the aqueous complexation of SO_4 and NTA

SO_4^{2-} is produced as Cd^{2+} is sorbed. This causes the distribution of SO_4^{2-} to mimic that of a conservative solute. Thus, while the sorption of Cd^{2+} is considerable, only NTA^{3-} increases above its source concentration.

The high equilibrium constant associated with reaction R3A implies that a significant level of cadmium is present in the form of $CdNTA^-$. Moreover, if the concentration of NTA^{3-} is increased in the source fluid, the equilibrium constraint will force the concentration of $CdNTA^-$ to be even greater. As $CdNTA^-$ is increased, more Cd^{2+} is available through dissociation to counter the sorption process. Consequently, the addition of NTA^{3-} should enhance the mobility of Cd^{2+}.

This concept is demonstrated in Figure 12. The figure clearly illustrates the increase of Cd^{2+} in solution as the concentration of NTA^{3-} is raised in the source fluid. The increase in soluble $Cd^{2+}$is due only to the presence of more $CdNTA^-$, and not from desorption. In fact, the more Cd^{2+} in solution, the higher the concentration of sorbed Cd^{2+} because the isotherm is linear.

Sorption and Aqueous Reactions: An Example in Two Dimensions

Inasmuch as SATRA-CHEM can simulate transport in two dimensions, the trends discussed above may be demonstrated in this perspective as well. As an example, the chemical system involving reactions R1 through R3 depicted in Figure 10 (K_{12} = 0.5, K_{14} = 1.0, F = 0.25, with inflow concentrations of C_1 = 2.0, C_2 = 1.0 and C_4 = 1.0) is applied to a two-dimensional, areal, flow field with steady-state hydraulic heads. This requires a new finite-element grid and boundary conditions (Figure 13).

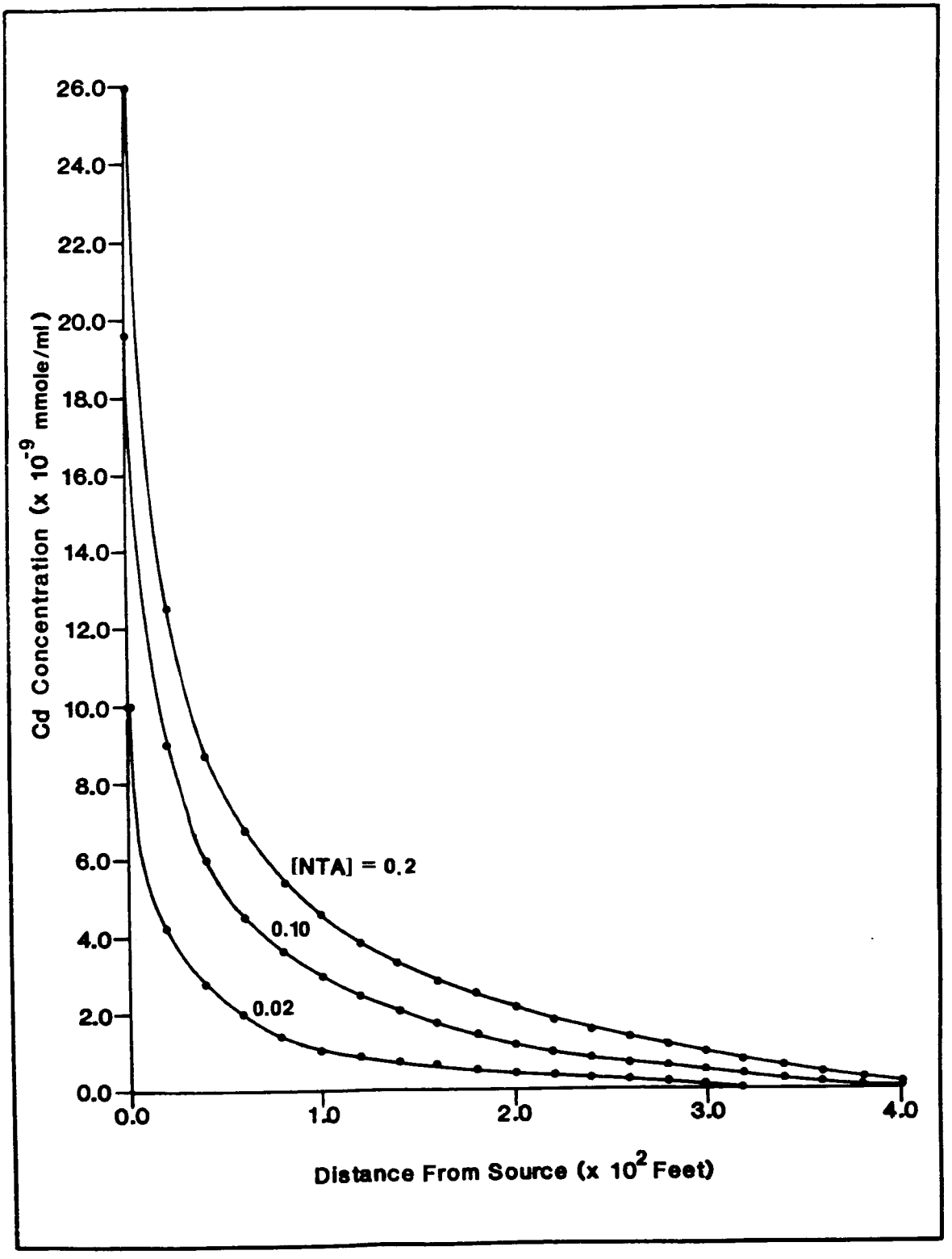

Figure 12. Distributions of Cd in solution as a function of the concentration of NTA in the source fluid

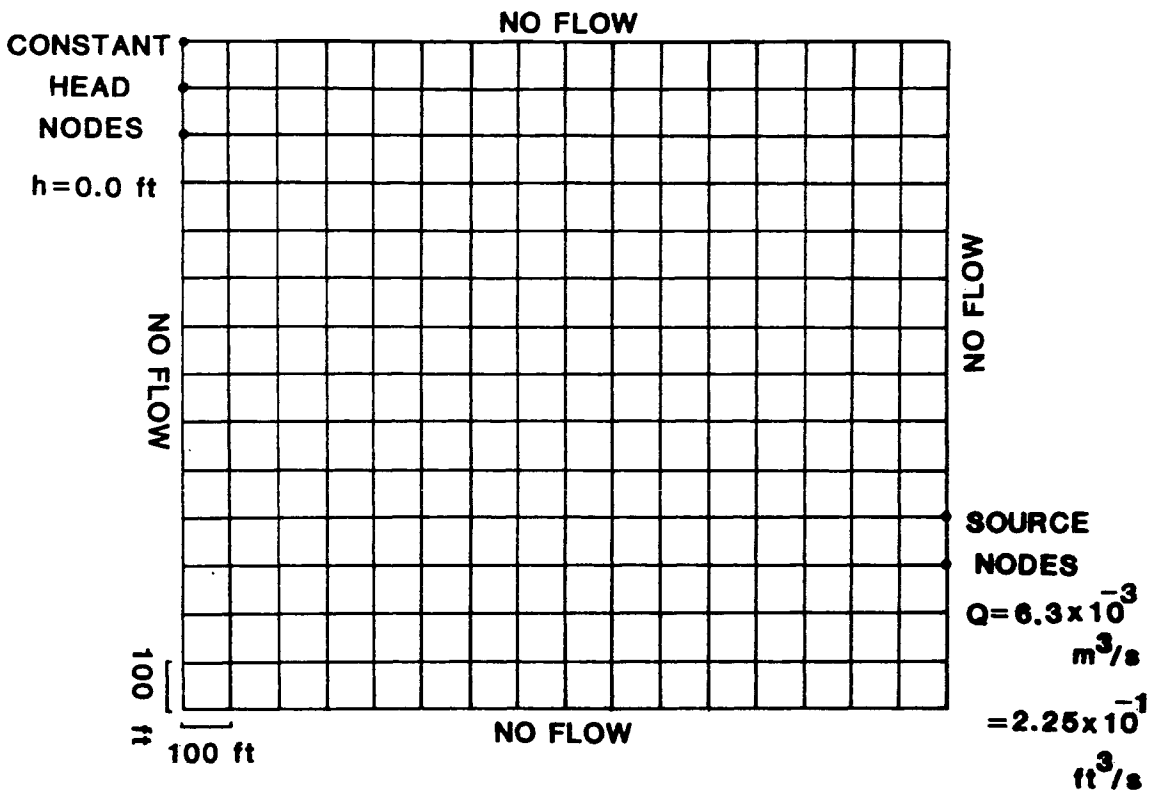

Figure 13. Finite-element grid and boundary conditions for two-dimensional transport simulations

Most of the physical parameters listed in Table 1, however, remain the same; only the values of dispersivity are new: longitudinal (α_L) = 30 feet, and transverse (α_T) = 5 feet.

In this case, flow is initiated at two adjacent nodes along the boundary through a specified volumetric flux. Both the flux and the source concentrations remain constant and continuous throughout the simulation. On the opposite boundary, three nodes have constant heads set at zero. The remainder of the boundary nodes constitute a no-flow boundary. The time-step interval is the same as in the runs above (excluding the Cd^{2+} example).

Figures 14 through 22 show in plan view the progression of all three reactant fronts through time. The results follow the anticipated pattern of concentration distribution based on the discussion of Figure 10 above.

Equilibrium Ion Exchange and Aqueous Reactions

The performance of the model regarding the transport of this hybrid chemical system can also be demonstrated with a few examples. The results of experimental runs are presented in which the physical constraints and boundary conditions are the same as those employed in all one-dimensional simulations discussed above (excluding the Cd^{2+} example); only the reactions and initial conditions differ. Here, the porous medium is initially saturated with fluid containing the following reactant concentrations: $C_1 = 0.0$, $C_2 = 0.0$ and $C_3 = 1.0$. The electrostatic balance is maintained by the presence of an additional non-reactive species. In the source fluid, concentrations are the opposite

Most of the physical parameters listed in Table 1, however, remain the same; only the values of dispersivity are new: longitudinal (α_L) = 30 feet, and transverse (α_T) = 5 feet.

In this case, flow is initiated at two adjacent nodes along the boundary through a specified volumetric flux. Both the flux and the source concentrations remain constant and continuous throughout the simulation. On the opposite boundary, three nodes have constant heads set at zero. The remainder of the boundary nodes constitute a no-flow boundary. The time-step interval is the same as in the runs above (excluding the Cd^{2+} example).

Figures 14 through 22 show in plan view the progression of all three reactant fronts through time. The results follow the anticipated pattern of concentration distribution based on the discussion of Figure 10 above.

Equilibrium Ion Exchange and Aqueous Reactions

The performance of the model regarding the transport of this hybrid chemical system can also be demonstrated with a few examples. The results of experimental runs are presented in which the physical constraints and boundary conditions are the same as those employed in all one-dimensional simulations discussed above (excluding the Cd^{2+} example); only the reactions and initial conditions differ. Here, the porous medium is initially saturated with fluid containing the following reactant concentrations: C_1 = 0.0, C_2 = 0.0 and C_3 = 1.0. The electrostatic balance is maintained by the presence of an additional non-reactive species. In the source fluid, concentrations are the opposite

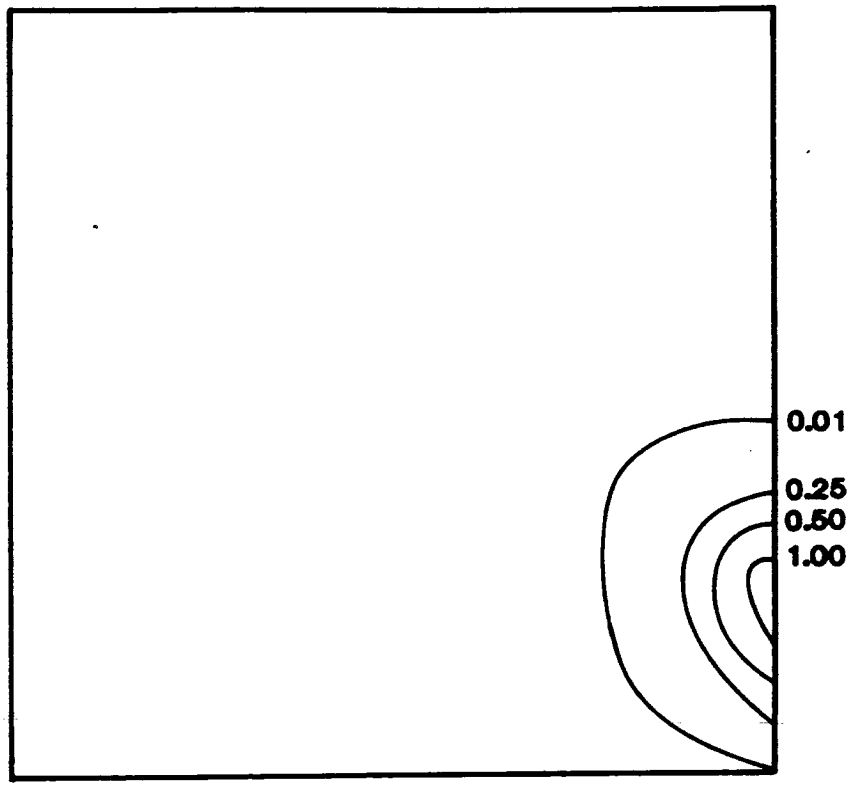

Figure 14. Two-dimensional distribution of C_1 after 1 time step (approximately 90 days). Transport contains sorption (R1, F = 0.25) and two aqueous complexations (R2, K_{12} = 0.5 and R3, K_{14} = 1.0)

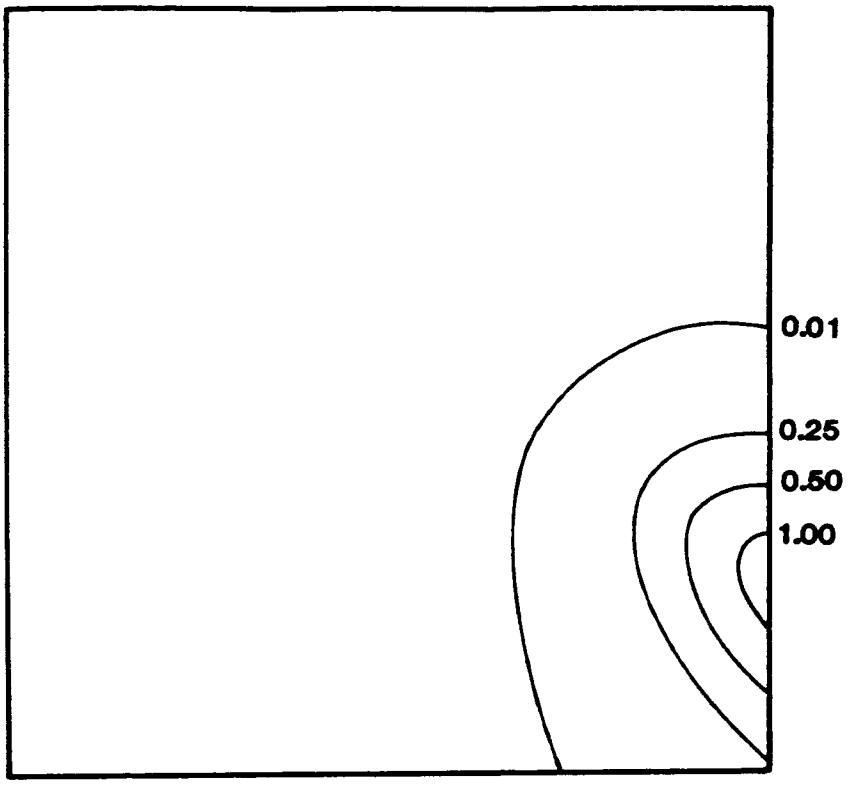

Figure 15. Two-dimensional distribution of C_2 after 1 time step

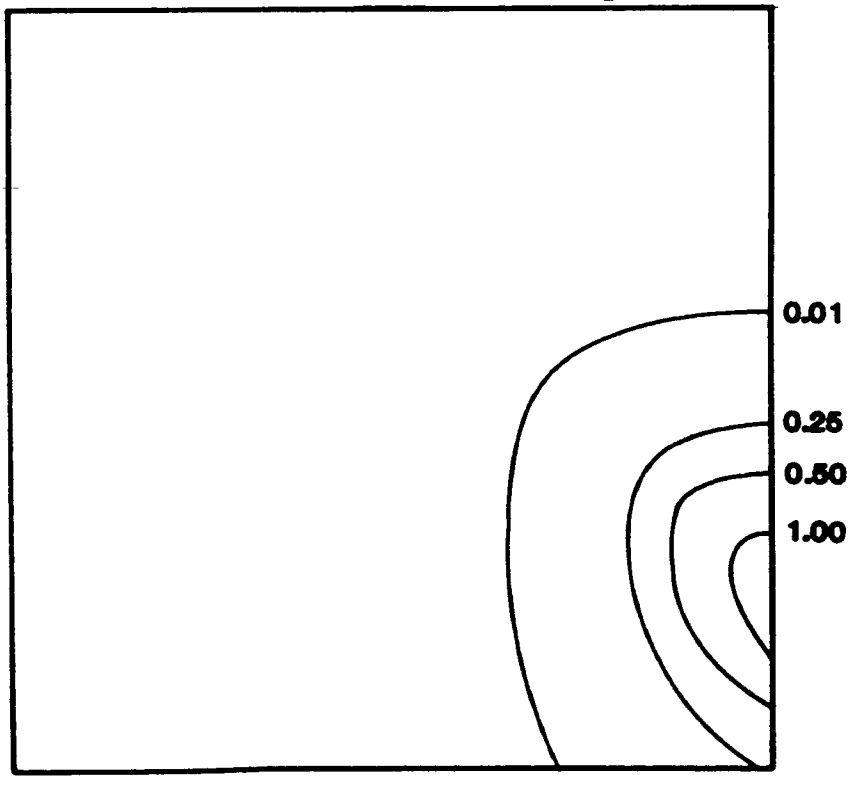

Figure 16. Two-dimensional distribution of C_4 after 1 time step

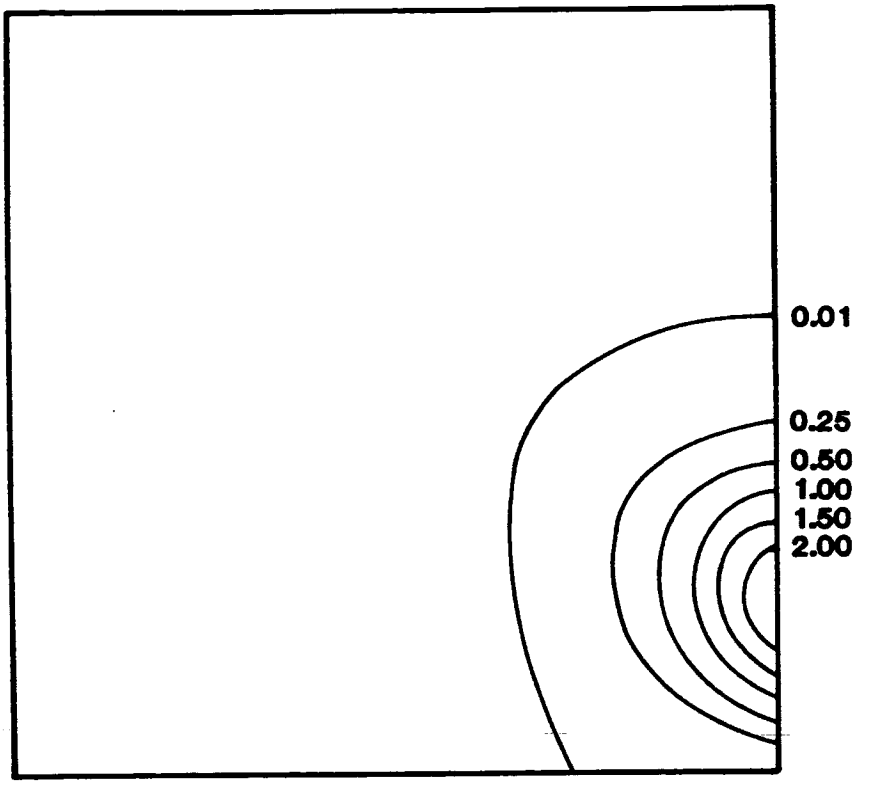

Figure 17. Two-dimensional distribution of C_1 after 5 time steps

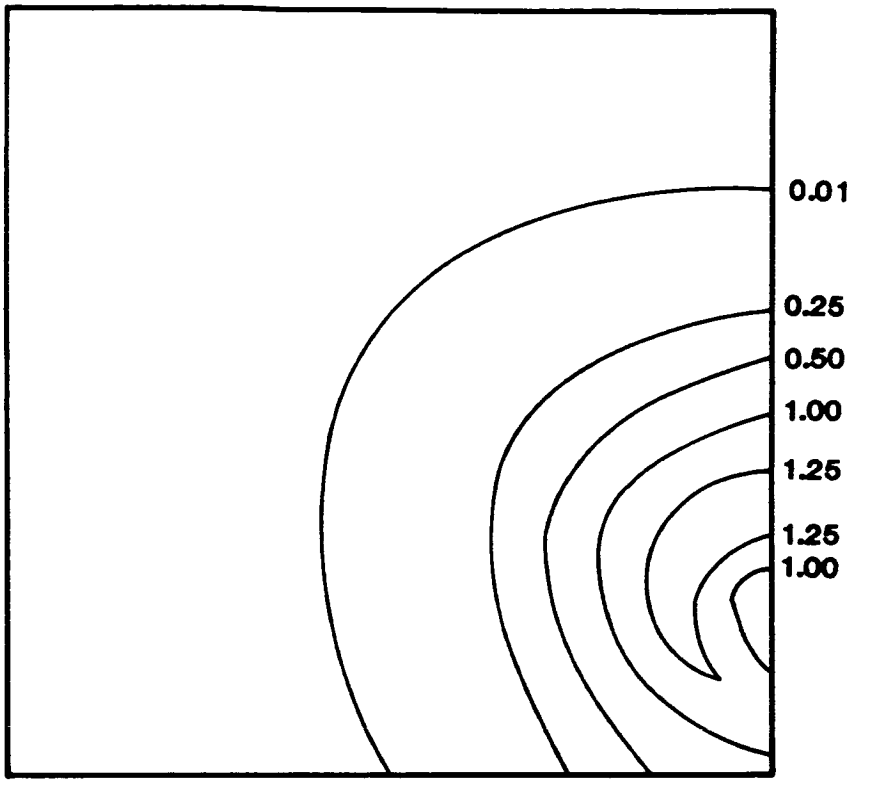

Figure 18. Two-dimensional distribution of C_2 after 5 time steps

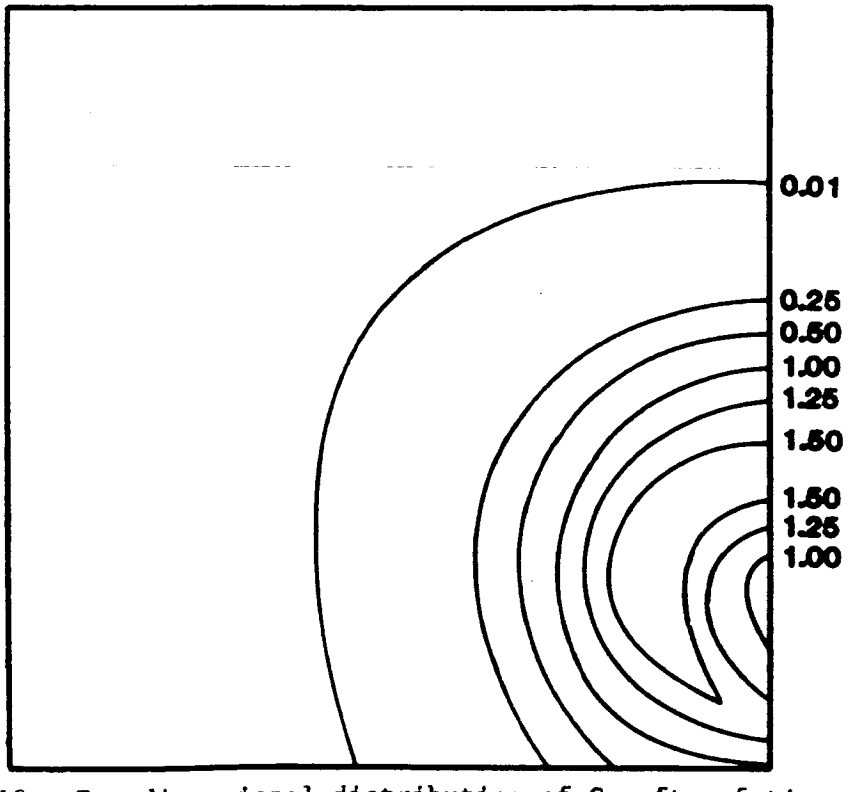

Figure 19. Two-dimensional distribution of C_4 after 5 time steps

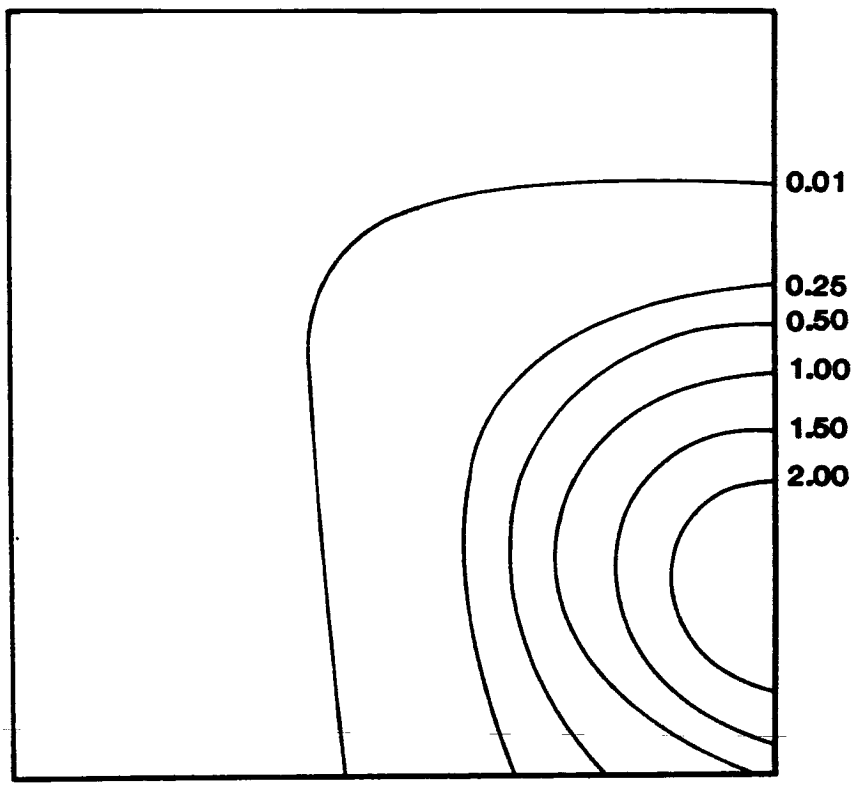

Figure 20. Two-dimensional distribution of C_1 after 20 time steps

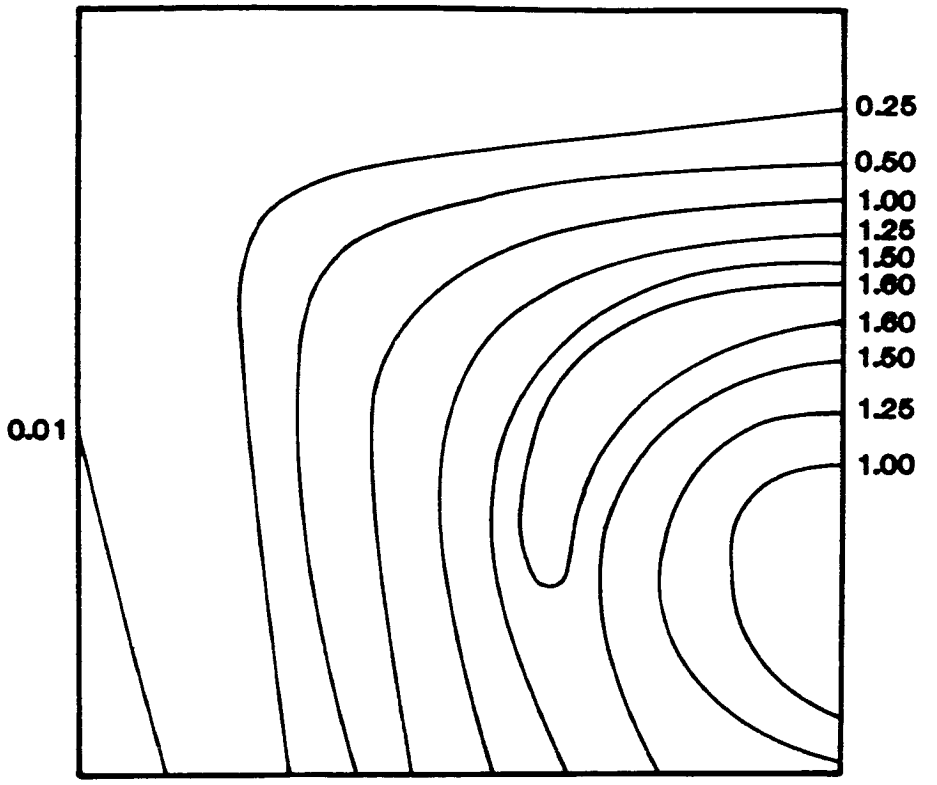

Figure 21. Two-dimensional distribution of C_2 after 20 time steps

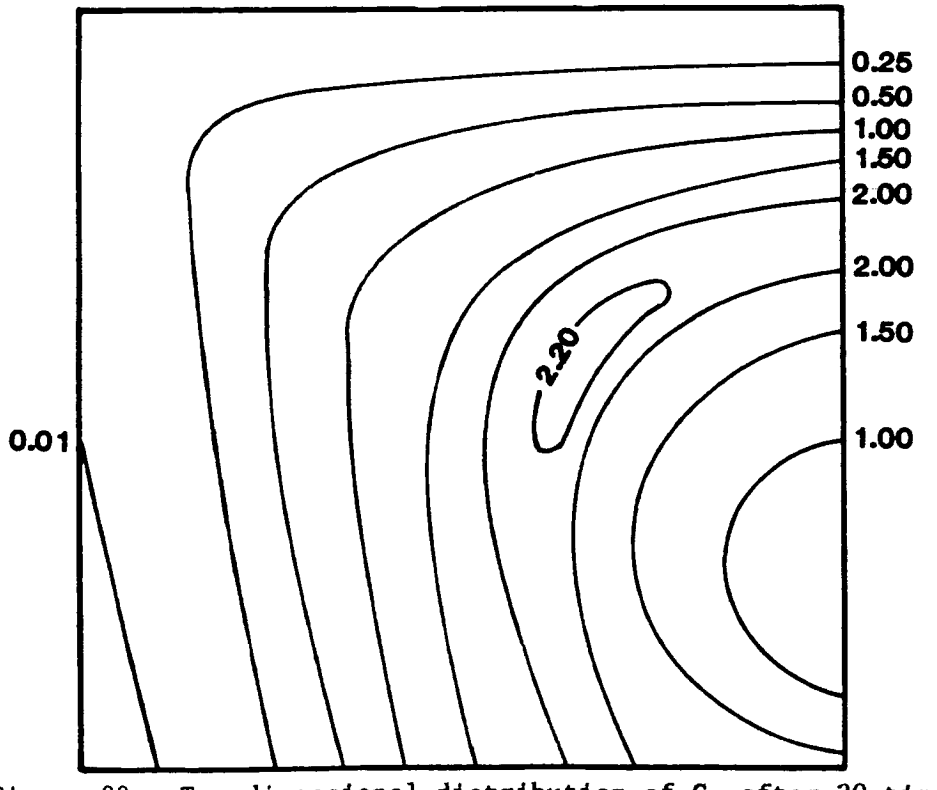

Figure 22. Two-dimensional distribution of C_4 after 20 time steps

of the background levels; specifically, $C_1 = 1.0$, $C_2 = 1.0$ and $C_3 = 0.0$.

Ion Exchange Alone

Figure 23 shows the concentration distributions for binary ion exchange without an accompanying homogeneous reaction. The results are after 15 time steps (approximately 7.5 years) with $K_{13}=1.0$ and $\bar{C}_T=0.02$. The transport of C_2 is included to indicate the distribution of a conservative solute.

Inasmuch as C_1 is constant in the inflow solution and equal to the level of C_3 initially present in the porous media, one may conclude that their sum is constant at every point and for all time (i.e., $C_T = C_1+C_3$). This relationship is valid because the total normality of the dissolved ionic species cannot be altered by the exchange process alone (Rubin and James, 1973), and this is supported by the results. Figure 23 shows that as C_1 increases, C_3 decreases equally such that their sum remains constant at 1.0. Note the addition of a simultaneous aqueous reaction to this chemical system will nullify the condition of constant C_T.

Apart from the Peclet number, the geometry of the exchanging C_1 front is a function of both the selectivity coefficient, K_{13}, and the exchange capacity of the media, $\bar{C}_T$. The effect of K_{13} on C_1 may be traced to the nature of the exchange isotherm. With C_T constant and R4 the only reaction, equations (33) and (35) can be combined to formulate an exchange isotherm for M_1 as follows:

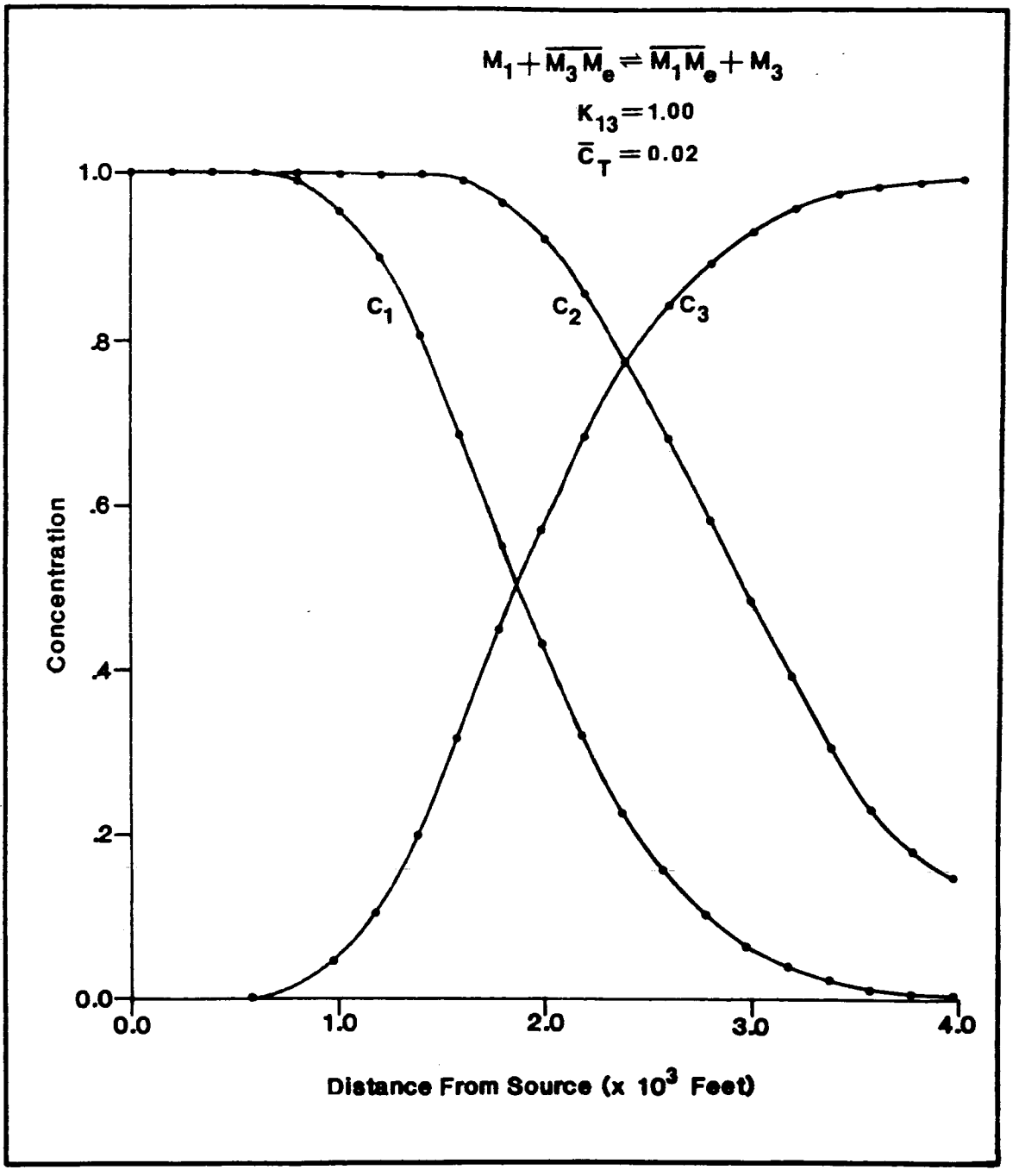

Figure 23. Transport with binary ion exchange (R4, K_{13} = 1.0) and a conservative solute (C_2) after 15 time steps (approximately 7.5 years); $\bar{C}_T$ =0.02

$$\bar{C}_1 = \frac{K_{13}C_1\bar{C}_3}{C_3}$$

$$= \frac{K_{13}}{C_3}\left[\bar{C}_T - \left(\frac{K_{13}C_1\bar{C}_T}{K_{13}C_1 + C_3}\right)\right]$$

$$= \frac{K_{13}\left(\frac{C_1}{C_T}\right)\bar{C}_T}{1 + (K_{13}-1)\left(\frac{C_1}{C_T}\right)}$$

$$= \frac{K_{13}C_1\bar{C}_T}{C_T + (K_{13}-1)C_1} \qquad (63)$$

Previous studies (e.g., Lai and Jurinak, 1972; Valocchi et al., 1981) have noted that the shape of isotherms derived similarly depend on whether K_{13} is less than, equal to, or greater than one.

Figure 24 shows the resulting isotherms when equation (63) is solved using values of K_{13} equal to 10.0, 1.0, and 0.1. The corresponding C_1 profiles after 15 time steps with $\bar{C}_T = 0.02$ are found in Figure 25. When $K_{13} = 1.0$, the isotherm is linear and the retardation of the exchanging front is constant. In terms of reaction R4 and the chemical-relation equation (33), this implies that $\bar{C}_1$ replaces $\bar{C}_3$ at a constant rate as a function of solute concentration. When $K_{13}<1.0$, the isotherm is concave and the corresponding front is more dispersed because significantly larger values of C_1 are associated with a given level of $\bar{C}_1$. In this case, $\bar{C}_1$ replaces $\bar{C}_3$ initially at a reduced rate that continually increases as C_1 rises. As a result, at low concentrations M_1 is mostly in the solute phase and able to travel farther. When

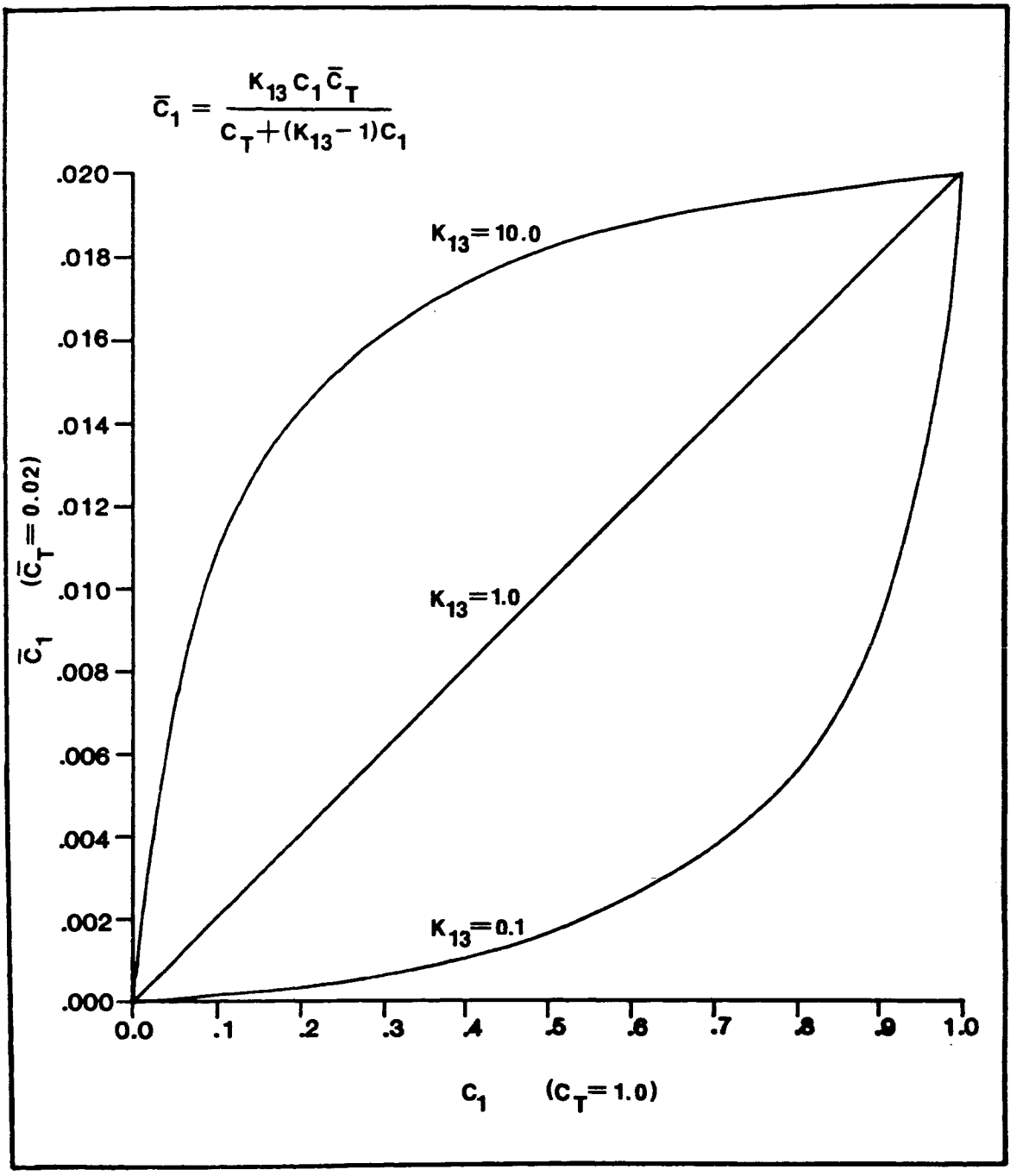

Figure 24. Exchange isotherms for M_1 as a function of the selectivity coefficient, K_{13}

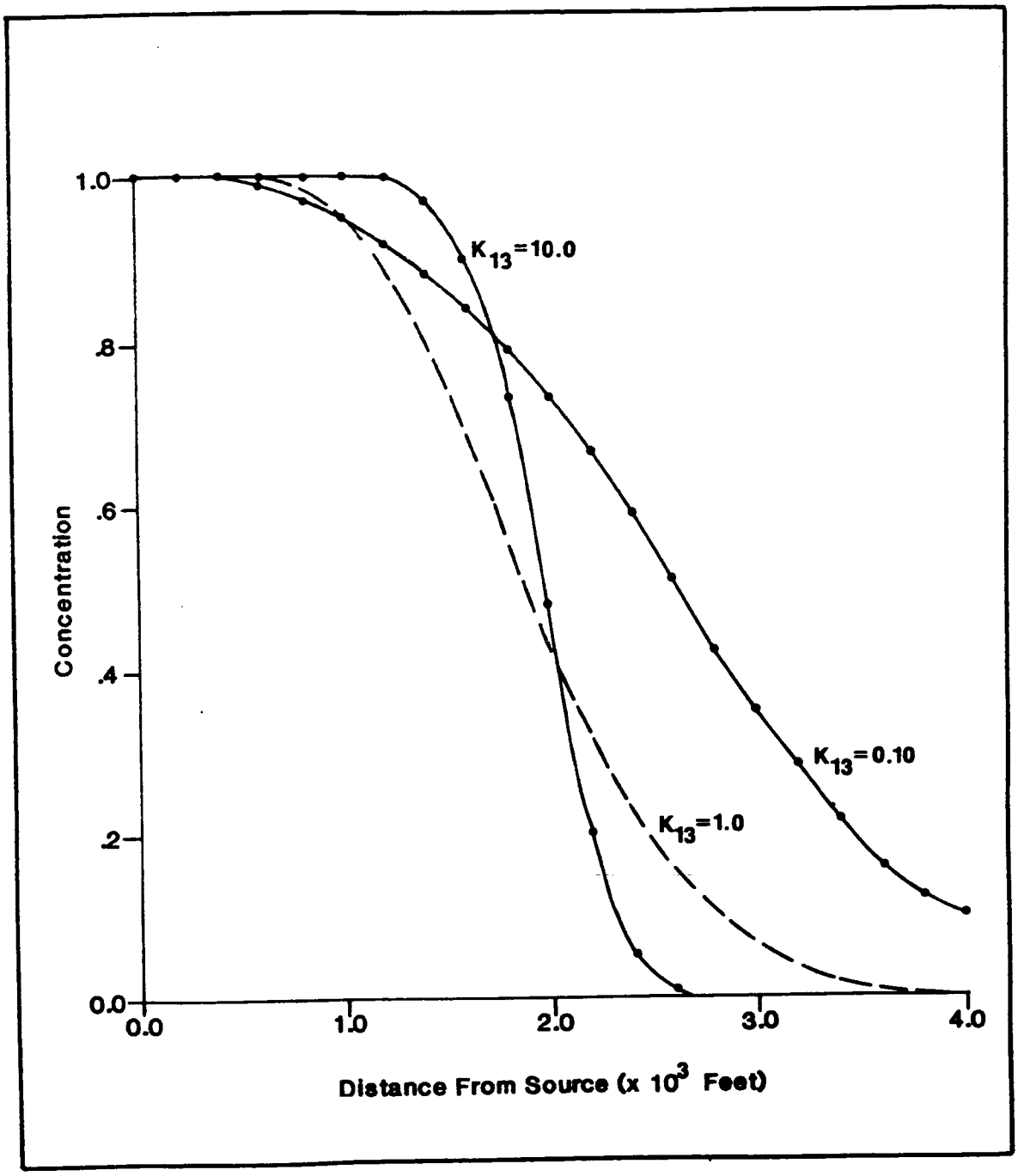

Figure 25. The effect of the selectivity coefficient, K_{13}, on the distribution of the exchanging C_1 front

$K_{13}>1.0$, the isotherm is convex causing M_1 to be sorbed preferentially to M_3. The result is a relatively sharp front.

The effect of exchange capacity on the exchanging solute distribution has been demonstrated previously by Rubin an James (1973). In general, the greater the value of $\bar{C}_T$, the more retarded the exchanging front. A higher $\bar{C}_T$ means the sorbed phase constitutes an increased proportion of the tenad mass as it travels through the system. Figure 26 shows the distribution of C_1 following two runs of 18 time steps with $\bar{C}_T = 0.02$ and $\bar{C}_T = 0.20$. The results are for ion exchange alone ($K_{13} = 1.0$); however, the presence of an additional aqueous equilibrium reaction would not alter this trend.

As in the case of linear sorption, an analytical solution is available to check the results produced by the model in Figure 26. For the special case of $K_{13} = 1.0$, the exchange isotherm is linear, and equation (62) applies. Figure 27 shows the analytical solution as smooth curves and the corresponding numerical results plotted as points. The model results agree well with the exact solution for both values of exchange capacity.

Ion Exchange and One Aqueous Reaction

Figure 28 shows the results produced by the model when both reactions R4 and R5 occur simultaneously. The profiles represent solute concentrations after 11 time steps when $\bar{C}_T = 0.2$ and $K_{12} = K_{14} = 1.0$. As in the similar case of linear sorption, both C_2 and C_3 increase above their respective boundary conditions.

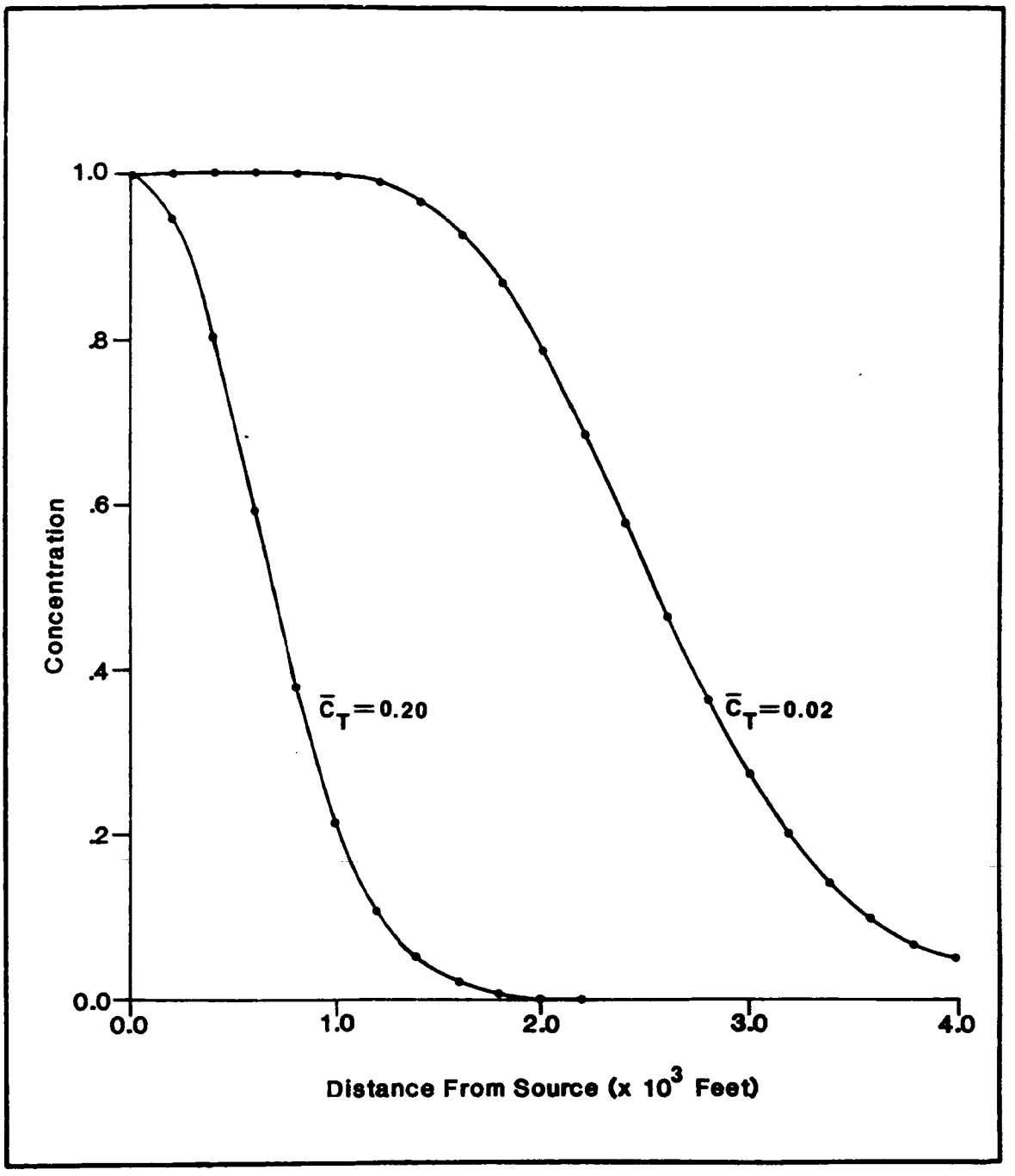

Figure 26. The effect of the exchange capacity, $\bar{C}_T$, on the distribution of the exchanging C_1 front

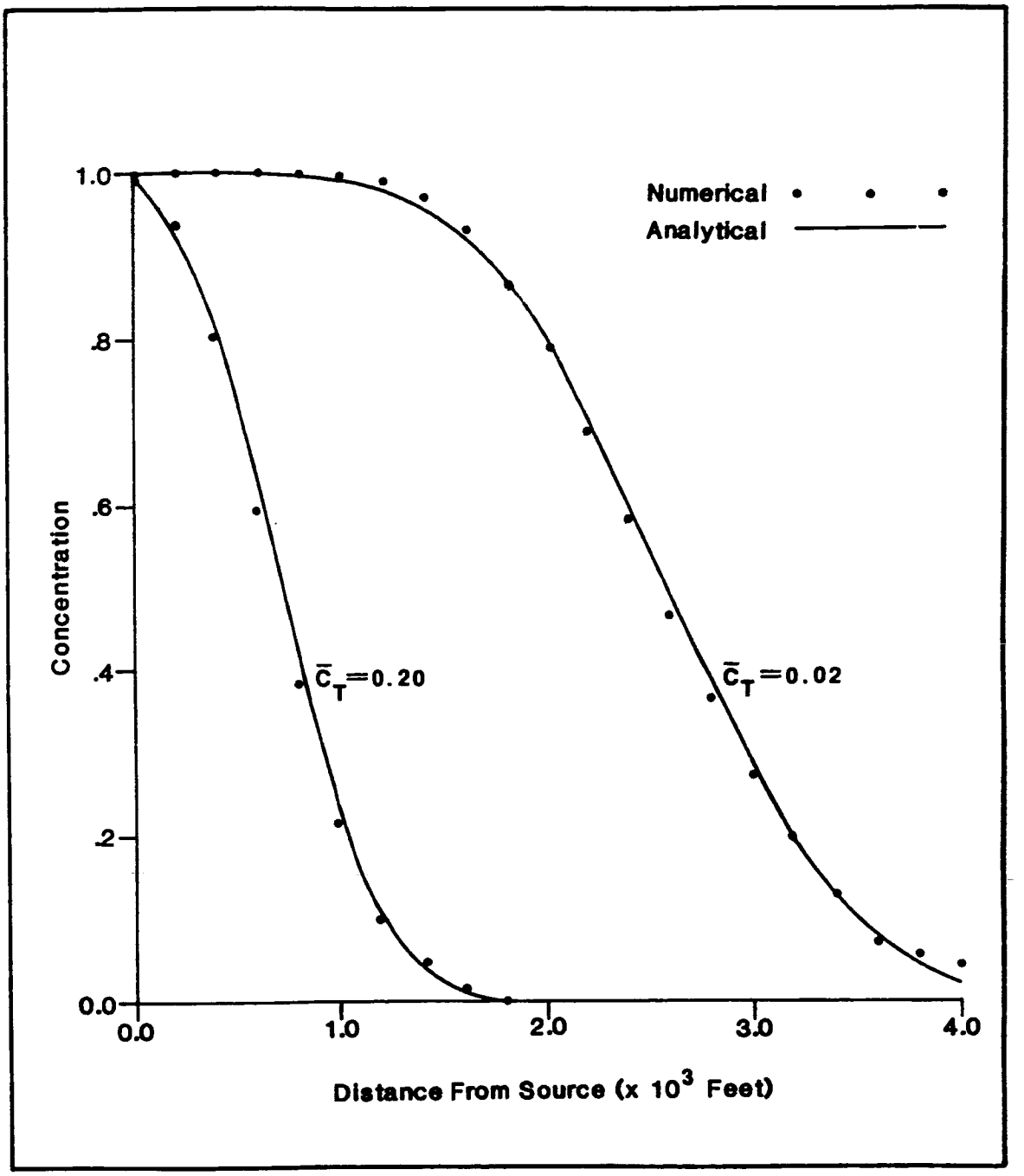

Figure 27. Numerical versus analytical solutions when comparing the effect of different exchange capacities on the distribution of the exchanging C_1 front

Figure 28 illustrates the cyclical pattern of sorption and dissociation typical in hybrid chemical systems as defined in this study: the sorption of M_1 through the exchange of M_3 in R4, leads to the production of both M_1 and M_2 through the dissociation of M_1M_2 in R5. Additional M_1 leads to an increase in the proportion of $\bar{C}_T$ comprised of $\bar{C}_1$; consequently, more M_3 is in solution than would be otherwise. Note the rise in C_3 above its background concentration is due to the total dissolved amount of $\{M_1\}$ in the system. In this case, the additional source of $\{M_1\}$ is the M_1M_2 complex; however, a distribution of C_3 similar to that shown in Figure 28 would also result if ion exchange (R4) occured alone, and the inflow concentration of M_1 was higher than the initial background level of C_3 (i.e., $C_T \neq$ constant). The important point is that the more dissolved M_1 there is in the system, regardless of origin, the more M_1 is sorbed. This, in turn, leads to an increase of M_3 in solution because $\bar{C}_T$ is constant. Therefore, the cause of the C_3 peak is not the same as that for C_2. The peak in the latter concentration distribution remains at the point of maximum difference between the exchanging (sorbing) front and an equivalent conservative distribution. However, for both M_2 and M_3, the peak concentrations are governed by the equilibrium constraints and the exchange capacity of the media.

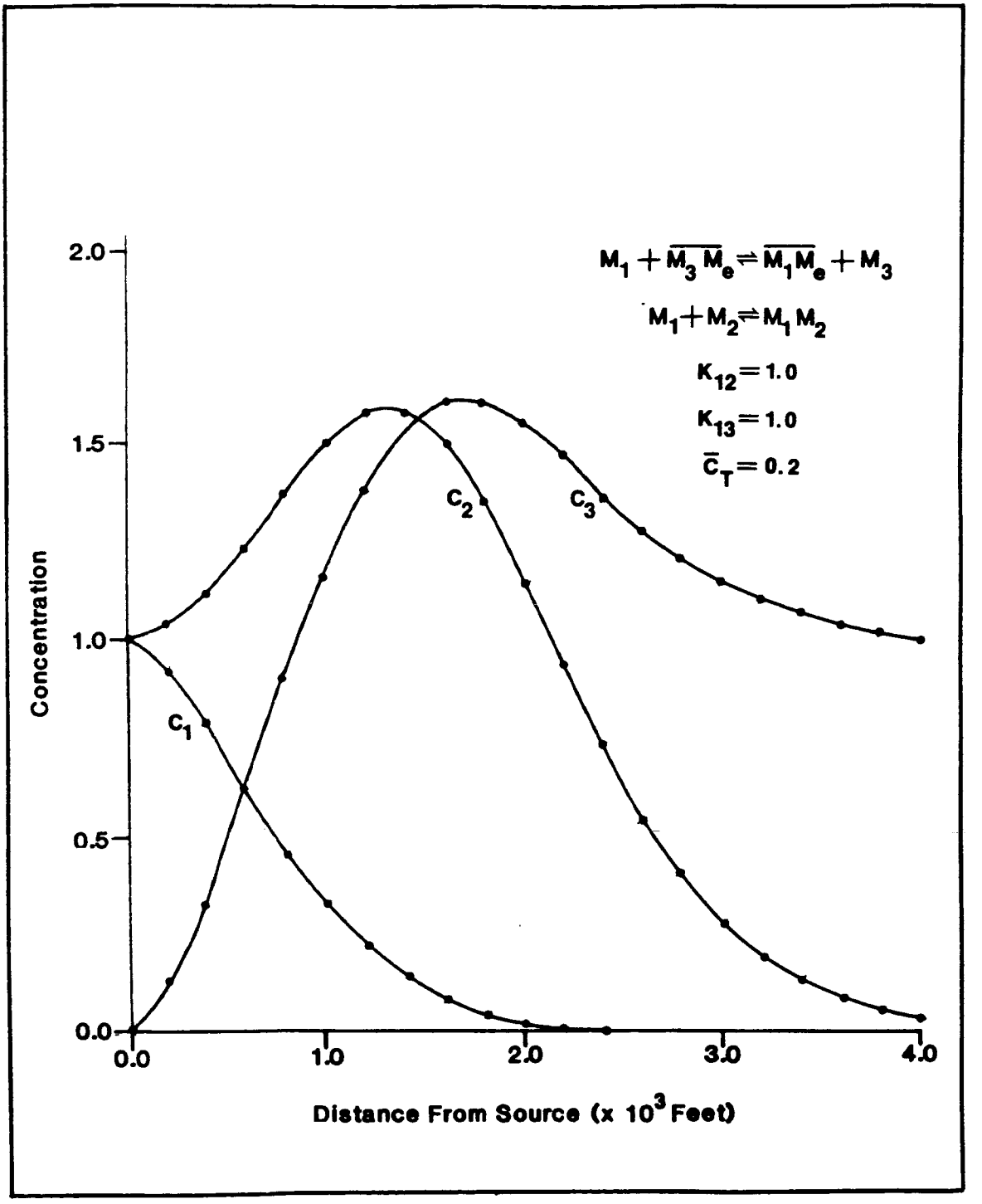

Figure 28. Transport with binary ion exchange (R4, K_{13} = 1.0) and one aqueous equilibrium reaction (R5, K_{12} = 1.0) after 11 time steps (approximately 5.5 years)

DISCUSSION

The reactive transport methodology presented in this study provides a means of examining (1) the effects of advection/dispersion on the distribution of non-sorbing solutes in aqueous equilibrium-controlled reactions, and (2) the distribution of chemical species participating in aqueous equilibrium reactions with species that sorb. By simulating these reactive processes, results produced by the model demonstrate trends that have not appeared before in the hydrologic literature. Although previous studies (e.g., Jennings et al., 1981) have shown the effects of aqueous complexation on sorption, and thus imply the potential to produce results similar to those presented here. All of the transport examples above, with the exception of equilibrium sorption alone and binary ion exchange alone, offer new information on the distributions of reactive migrating solutes.

In introducing this methodology and the trends produced from various simulations, only some of the more fundamental reaction combinations, and thus the transport of only a limited number of species, may be examined using the current version of the model. Future versions may be made more verstile by employing some of the following modifications:

1. Include values other than one for the activity and stoichiometric coefficients. For the activity coefficients this involves determining the appropriate value either internally or externally of the program itself. DeBye-Huckel or Guntelberg approximations (Snoeyink and Jenkins, 1980) and the Davies equation (Strumm and Morgan, 1970) provide

values of activities as a function of temperature, pressure and ionic strength. Once activities are known, they are multiplied by the appropriate values of concentration in the chemical-relation equations (8), (9), (33) and (34). Stoichiometric coefficients also influence the chemical-relation expressions. In equations (8), (9), (33) and (34), the coefficients become exponents for the concentrations. Moreover, subsequent algebraic manipulations of these equations such as (20)-(23), must account for these changes as well.

2. Include the ability to simulate N additional aqueous equilibrium reactions where N is some arbitrary user-specified integer such as 10. This would be most feasible for the first chemical system involving linear sorption. The principal obstacle would be the assemblage of the N-degree polynomial (equation 32) and its solution.

3. Incorporate additional sorption reactions such that more than one chemical species may be sorbed simultaneously.

4. Incorporate the option of chemical kinetics through reaction-rate coefficients for some reactions as an alternative to the assumption of local chemical equilibrium.

These modifications will still not produce a model that can account for all possible chemical mechanisms a particular species may encounter during its migration through a ground-water system. As chemical complexity increases "one-step" approaches to reactive transport become more limiting, and "two-step" approaches appear more attractive. The successful simulation of a particular problem requires a trade-off between numerical and computational efficiency and chemical accuracy.

As a result, a set of criteria should be established prior to selecting a given approach. The most important criteria being the objective of the transport study, and the level of detail at which the results are to be presented. Additional criteria should involve the scale of the problem, particularly in terms of the number of nodes required to model adequately the area of interest; the type and number of reactions; the number of transported solutes; whether equilibrium or kinetic models are the most appropriate; and whether the input and/or assumed conditions can be verified.

SUMMARY AND CONCLUSIONS

The principal objectives of this thesis were to (1) introduce a general mathematical structure in which the mechanisms of sorption or ion exchange, coupled with aqueous equilibrium-controlled reactions, can be incorporated into advective-dispersive transport; and (2) use the simulated concentration distributions that result from these reaction combinations to understand some of the processes important in the simultaneous transport of several interacting solutes.

Two hybrid chemical systems were defined, each containing one tenad that simultaneously participates in both solid phase and aqueous reactions. The interrelationships among the reactions produced a strongly nonlinear partial differential equation describing the transport of this tenad; and the solution required the tracking of all additional reactive tenads through linear transport equations. The nonlinear components were converted into two new variables that were incorporated into a general form of the advection-dispersion equation. The resulting equations were solved by modifying an existing two-dimensional finite-element computer code. By combining the mathematics of equilibrium chemistry such that only one nonlinear equation is developed, this methodology provides an efficient means of solving for single species sorption in hybrid chemical systems as defined in this study.

The results of several example simulations enabled the following conclusions to be drawn:

1. A reactant chemical species participating in an aqueous equilibrium-controlled reaction will have higher concentrations along the solute front than an equivalent conservative species, and the difference in concentration between the two species is a function of the equilibrium constant for the particular reaction.

2. Given two chemical species that react through equilibrium reactions: if one is concurrently removed from solution through either sorption or ion exchange, the other will show a corresponding increase in concentration as dictated by the equilibrium condition. The concentration increase, which may temporarily exceed the boundary conditions specified for that species, is a function of the linear sorption coefficient (or the exchange capacity of the media), the equilibrium constant, and the amount of elapsed time. The maximum level of increase is governed by the total dissolved tenad concentration of which the increasing reactant species is a part.

3. If another aqueous equilibrium reaction containing the same sorbing species is added to the system described above, the resulting concentration increase will be the greatest for the non-sorbing species participating in the reaction with the highest equilibrium constant.

4. Inasmuch as the reaction processes are active only along the solute front, the steady-state solution to reactive transport, as defined in this study, is the same as for a conservative solute, regardless of the nature or degree of chemical interaction.

5. In a chemical transport system defined only by binary ion exchange, the shape of the front is a function of the selectivity coefficient, K_{13}, and the exchange capacity of the media. If K_{13} is equal to 1.0, then the exchange isotherm is linear. When K_{13} is greater than 1.0, the isotherm is convex producing a sharper exchanging front. If K_{13} is less than 1.0, the isotherm is concave an the front is more dispersed. Increasing the total exchange capacity acts to retard the exchanging front.

6. As a result of the two-dimensional nature of the basic transport algorithm, the model is able to simulate in two dimensions all of the one-dimensional reaction systems described in this study.

APPENDIX A

NOTATION

A	A function of concentration; defined on page 26.
B	A function of concentration; defined on page 26.
C_1, C_2, C_3, C_4	Dissolved concentrations of arbitrary chemical species 1, 2, 3 and 4 in the aquifer $[ML^{-3}]$.
$C_1^*, C_2^*, C_3^*, C_4^*$	Dissolved concentrations of arbitrary chemical species 1, 2, 3 and 4 in the source fluid $[ML^{-3}]$.
C_{12}, C_{14}	Dissolved concentrations of chemical compounds comprised of C_1, C_2 and C_4 in the aquifer $[ML^{-3}]$.
C_{12}^*, C_{14}^*	Dissolved concentrations of chemical compounds comprised of C_1^*, C_2^*, and C_4^* in the aquifer $[ML^{-3}]$.
$\bar{C}_1, \bar{C}_3$	Adsorbed concentrations of arbitrary chemical species 1 and 3 $[MM_s^{-1}]$.
C_T	Total dissolved concentration in the system $[ML^{-3}]$.
$\bar{C}_T$	Total exchange capacity of the medium $[MM_s^{-1}]$; defined in equation (35).
$\underline{\underline{D}}$	Hydrodynamic dispersion tensor $[L^2t^{-1}]$.
f	Adsorbate source in solute mass-balance relationships ships $[ML^{-3}t^{-1}]$; defined in equations (2) and (3).
f_1, f_2	Functions of concentration; defined in equations (52)-(53).

f_s	Solute-mass adsorption rate per unit mass of solid matrix (adsorbate flux) $[M_s M^{-1} t^{-1}]$; defined on page 7.
F	Linear sorption coefficient which represents the ratio of solute mass sorbed per unit solid mass to solute mass per unit volume of water $[L^3 M_s]$.
g	A function off concentration; defined in equaton (51).
G	A function of concentration; defined in equation (29).
h	Hydraulic head [L].
H	A function of concentration; defined in equation (28).
k	Time step indicator.
k_1, k_2	Coefficients in the nonlinear mass-balance equation that describe the nature of chemical interaction; defined specifically for equilibrium sorption and aqueous complexation on page 18, and for binary ion exchange and aqueous complexation in equations (60)-(61).
$\underline{\underline{K}}$	Hydraulic conductivity tensor $[Lt^{-1}]$.
K_{12}	Chemical equilibrium constant for aqueous equilibrium reactions R2 and R5 $[L^3 M^{-1}]$; defined in equations (8) and (34).
K_{13}	Chemical equilibrium constant (selectivity coefficient) for the binary ion exchange reaction R4 [1]; defined in equation (33).
K_{14}	Chemical equilibrium constant for the aqueous equilibrium reaction R3 $[L^3 M^{-1}]$; defined in equation (9).
K_d	Equilibrium distribution coefficient; same as the linear sorption coefficient, F, defined above.
L	Length
L(U)	Linear operator representing the fundamental advective-dispersive components with respect to concentration U; defined in equation (6).

M	Mass of fluid or solute.
M_s	Mass of solid.
M_1, M_2, M_3, M_4	Masses of arbitrary chemical species 1, 2, 3 and 4 which are participants in reactions R1-R5.
M_1M_2, M_1M_4	Masses of chemical compounds, defined in reactions R2, R3 and R5, which are comprised of M_1, M_2 and M_4
$\bar{M}_1$, $\bar{M}_3$	Sorbed masses of arbitrary chemical species 1 and 3 which are components of reactions R1 and R4.
$\bar{M}_e$	Mass of arbitrary cation exchanger in reaction R4.
$\bar{M}_x$	Reactive surface of solid grain in reaction R1.
Q	Volumetric fluid source (volume of fluid injected per time per volume of aquifer) $[t^{-1}]$.
R	Retardation factor with respect to the average linear velocity of a sorbing solute.
Δt	Time step increment.
U,V,W	Functions of concentration in the aquifer defined in equations (13)-(15) and (44)-(47).
U^*,V^*,W^*	Functions of concentration in the source fluid.
α_L	Longitudinal dispersivity [L].
α_T	Transverse dispersivity [L].
$\underline{\beta}$	Coefficient matrix that contains the advective contributions for the numerical discretization of the basic transport equations.
$\underline{\chi}$	Coefficient matrix for the time derivative in the in the numerical discretization of the basic transport equations.
ϵ	Porosity [1]
$\underline{\lambda}$	Coefficient matrix that contains the dispersive components in the numerical discretization of the basic transport equations.
ρ	Fluid density $[ML^{-3}]$.

ρ_b	Bulk density $[ML^{-3}]$.
ρ_s	Solid-grain density $[M_s L^{-3}]$.
ϕ_j	Spatial basis function for node j.
Φ	Inverse of the retardation factor, R.
$\psi(x,y,t)$	Exact value of the dependent variable.
$\hat{\psi}(x,y,t)$	Approximate value of the dependent variable.
$\underline{\omega}$	Vector of nodal source contributions including the nonlinear terms in k_2.
$\underline{\nabla}$	Two-dimensional vector differential operator $(\frac{\partial}{\partial x}, \frac{\partial}{\partial y})$.

APPENDIX B

FORMATED INPUT DATA

This appendix contains the basic information for creating the formated data set necessary to run the model SATRA-CHEM version V05842D. The text below is modified from the chapter, "Running SATRA Simulations", found in Voss (n.d.).

The model generally requires two files of input data. The first, UNIT 5, contains both the aquifer and simulation control parameters, as well as the boundary conditions specified by the user for a given problem. The second file, UNIT 55, contains the initial conditions, and is only required for cold-starts of the model (i.e., for the first time step of the simulation). The option to restart (warm-start) is controlled by the parameters IREAD and ISTORE in DATASET 3 of the UNIT 5 file. ISTORE allows the final results of a simulation to be stored in a form directly usable as UNIT 55 data for future restarts.

List of Input Data for UNIT 5

DATASET 1: Input Data Heading (one card)

Variable	Format	Description
SIMULA	2A6	For areal transport simulation, write "SATRA AREAL SOLUTE TRANSPORT" beginning in the first column. For cross-sectional solute transport simulation, write "SATRA CROSS-SECTIONAL SOLUTE TRANSPORT" beginning in the first column.

DATASET 2: Output Heading (one card)

Variable	Format	Description
TITLE	80A1	First line of a heading for the input data set.

DATASET 3: Simulation Control Numbers (one card)

Variable	Format	Description
NN	I5	Exact number of nodes in finite element mesh.
NE	I5	Exact number of elements in finite element mesh.
NBI	I5	Full bandwidth of global banded matrix. NBI is equal to one plus twice maximum difference in node numbers in the element containing the largest node number difference in the mesh. This number is critical to computational efficiency, and should be minimized by careful numbering of the nodes. Setting NBI too small causes SATRA to automatically print out the correct value and stop.
NPINCH	I5	Exact number of pinch nodes in the finite element mesh.
NHBC	I5	Exact number of nodes at which hydraulic head is a specified constant value or function of time.
NC1BC NC2BC NC4BC	I5 I5 I5	Exact number of nodes at which the concentrations (C_1, C_2, C_3 (or C_4) respectively, are. specified constant or a functon of time.
NSO	I5	Exact number of nodes at which a fluid source/ sink is a specified constant value or function of time.
ISSTAT	I5	Set to 0 for simulation with TRANSIENT groundwater flow. Set to +1 for simulation of STEADY-STATE solute transport.
IREAD	I5	To read initial condition data (UNIT 55) for cold start (first time step of a simulation), set to +1. To read initial condition data (UNIT 55) for simulation restart (data which has previously been stored by SATRA on UNIT 66), set to -1.
ISTORE	I5	To store results of final time step on UNIT 66 for later use as initial conditions on a restart, set to +1. To cancel storage of final time step, set to 0.

DATASET 4: Temporary Card (one card)

Variable	Format	Description
GNU	D15.0	Hydraulic head boundary condition 'leakance' factor. A high value causes SATRA simulated head and specified head values at specified head nodes to be equal in all significant figures. A low value causes smulated heads to deviate significantly from specified values. The ideal value of GNU causes simulated and specified heads to match in the largest four or five significant figures only, and deviate in the rest. GNU is entirely a numerical artifact which will eventually be eliminated from input data and calculated automatically. Currently, user trial-and-error is required to determine an ideal GNU value for a given simulation. An initial guess of 0.01 is suggested.

DATASET 5: Spatial Control Parameter (one card)

Variable	Format	Description
UP	F10.0	Fractional upstream weight for stabilization of oscillations in results due to highly advective transport or unsaturated flow. UP may be given any value from 0.0 to +1.0. UP = 0.0 implies no upstream weighting (Galerkin method). UP = 0.5 implies 50% upstream weighting. UP = 1.0 implies full (100%) upstream weighting. Warning: upstream weighting increases the local effective longitudinal dispersivity of the simulation by approximately (UP.(ΔL)/2) where ΔL is the local distance between nodes along the direction of flow. Note that the amount of this increase varies from place to place depending on flow direction and element size. In order to guarantee a spatially oscillation-free transport simulation, the mesh must be designed fine enough, and/or, the value, UP, must be great enough so that the following condition holds approximately along every streamline: $\frac{1}{2}(\Delta L_{max}) \leq (UP \cdot (\Delta L)/2) + DSLFAC.DISPL(L)$ where where ΔL_{max} is the largest distance between nodes along the streamline ΔL is the local distance between nodes along the streamline. The product of DSLFAC and DISPL(L), is the longitudinal dispersivity, specified in DATASET 13 and 14. In other words, the total simulated longitudinal dispersivity (given by the sum of numerical weighting dispersivity and physical dispersivity) must be greater than one-half the maximum element length measured along the flow direction.

DATASET 6: Temporal Control Data (one card)

Variable	Format	Description
ITMAX	I10	Maximum allowed number of time steps in simulation.
DELT	D10.0	Duration of initial time step. [s]
TMAX	D10.0	Maximum allowed simulation time. [s] SATRA time units are always in seconds. Other time measures are related as follows: [min] = 60. [s] [h] = 60. [min] [d] = 24. [h] [week] = 7. [d] [mo] = 30.4375 [d] [yr] = 365.250 [d]
ITCYC	I10	Number of time steps in time step change cycle. A new time step size is begun at time steps numbered: 1+ n (ITCYC).
DTMULT	F10.0	Multiplier for time step change cycle. New time step size is: (DELT)(DTMULT).
NPCYC	I10	Number of time steps in pressure solution cycle. Hydraulic head is solve on time steps numbered: n(NPCYC), as well as on initial time step.
NUCYC	I10	Number of time step in concentration solution cycle. Transport equation is solved on time steps numbered: n(NUCYC) as well as on initial time step.
NPRINT	I10	Printed output is produced on time steps numbered: n(NPRINT), as well as on first and last time step.

DATASET 7: Printed Output Controls (one card)

Variable	Format	Description
KCOORD	I5	A value of -1 cancels printout of node coordinates, nodewise element thicknesses, and nodewise porosites and nodewise specific storativities. Set to 0 for full printout.
KELINF	I5	A value of -1 cancels printout of elementwise hydraulic conductivities and elementwise dispersivities. Set to 0 for full printout.
KINCID	I5	A value of -1 cancels printout of node incidences and pinch node incidences in elements. Set to 0 for full printout.
KPLOTH	I5	Set to a value of +1 for contourable printer plot of heads at all nodes in mesh. Set to -1 to cancel head plot.
KPLOTU	I5	Set to a value of +1 for contourable printer plot of concentrations or at all nodes in mesh. Set to -1 to cancel plot.
KVEL	I5	Set to a value of +1 to calculate and print fluid velocities at element centroids each time printed output is produced. Note that for non-steady state flow, velocities are based on results and heads of the previous time step and not on the newest values. A value of 0 cancels the option.
KBUDG	I5	Set to a value of +1 to calculate and print a fluid volume budget and solute mass budget each time printed output is produced. A value of 0 cancels the option.

DATASET 8: Iteration Controls (one card)

Variable	Format	Description
ITRMAX	I10	Maximum number of iterations allowed per time step to resolve non-linearities. Set to a value of +1 for non-iterative solution.
RHMAX	D10.0	Absolute iteration convergence criterion for head solution. Head solution has converged when largest head change from the previous iteration's solution of any node in mesh is less then RHMAX. May be left blank for non-iterative solution.
RUMAX	D10.0	Absolute iteration convergence criterion for transport solution. Transport solution has converged when largest concentration change from the previous iteration's solution of any node in mesh is less than RUMAX. May be left blank for non-iterative solution.
RTOL	D10.0	Absolute iteration convergence criterion for Newton-Raphson iteration procedure.
MAXITR	D10.0	Maximum number of iterations for Newton-Raphson iteration procedure.

DATASET 9: Simulation Control Identifiers

Variable	Format	Description
NCONT	I2	Number of chemical constituents involved in the simulation (e.g., if C_1, C_2 and C_4 are transported, NCONT = 3).
ISORB	I5	Adsorption indicator. A value of +1 implies the simulation involves linear sorption (i.e., FF>0 in DATASET 9). A value of 0 implies no exchange occurs.
IEXCH	I5	Ion exchange indicator. A value of +1 implies the simulation involves binary ion exchange. A value of 0 implies no exchange occurs.
IEQLIB	I5	Equilibrium chemistry indicator. A value of +1 implies the simulation involves at least one aqueous equilibrium chemical reaction. A value of 0 implies no aqueous reactions take place. If the simulaiton involves just sorption or just ion exchange, IEQLIB = 0 even though the reactions are technically in equilibrium.

DATASET 10: Fluid, Solid Matrix and Solute Properties (one card)

Variable	Format	Description
SIGMAW	D10.0	Fluid diffusivity, σ_w. Represents molecular diffusivity of solute in pure fluid. [L^2 /s].
RHOS	D10.0	Density of a solid grain, ρ_s, for sorption calculations. [M/L^3]. (Need be specified only if SORBL≠0).
DECAY	D10.0	Decay rate (first order) of solute, γ [M_s/s]. $(\partial C/\partial t) = -\gamma C$. Set to zero for no decay.
FF	D10.0	Linear sorption constant, F. Relates relative concentrations between solid and liquid phase for a particular chemical constituent. Set to positive value when ISORB>0 (DATASET 8).
CBART	D10.0	Total exchange capacity of the porous media, $\bar{C}_T$. Set to positive value when IEXCH>0 (DATASET 8).
EQCSTU	D10.0	Chemical equilibrium constant for reactions R2 and R5 (see thesis text). If either of these reactions is simulated, a positive value is required here and for IEQLIB (DATASET 8).
EQUCSTV	D10.0	Chemical equilibrium constant for reactions R3 and R4. If either of these reactions is simulated, a positive value is required here and for IEQLIB (DATASET 8).

DATASET 11: Scale Factor for Nodewise Data (one card)

Variable	Format	Description
SCALX	D10.0	The scaled x-coordinates of nodes in DATASET 12 are multiplied by SCALX in SATRA-CHEM. May be used to change from map to field scales, or from English to SI units. A value of 1.0 gives no scaling.
SCALY	D10.0	The scaled y-coordinates of nodes in DATASET 12 are multiplied by SCALY in SATRA-CHEM. May be used to change from map to field scales, or from English to SI units. A value of 1.0 gives no scaling.
SCALTH	D10.0	The scaled element (mesh) thicknesses at nodes in DATASET 12 are multiplied by SCALTH in SATRA-CHEM. May be used to easily change entire mesh thickness or to convert English to SI units. A value of 1.0 gives no scaling.
PORFAC	D10.0	The scaled nodewise porosities of DATASET 12 are multiplied by PORFAC in SATRA-CHEM. May be used to easily assign a constant porosity value to all nodes by setting PORFAC = porosity and all POR(II) = 1.0 in DATASET 12.
STOFAC	F10.0	The scaled nodewise specific storativities of DATASET 12 are multiplied by STOFAC in SATRA-CHEM. May be used to easily assign a constant storativity value to all nodes.

DATASET 12: Nodewise Data (one card for each of NN nodes)

Variable	Format	Description
II	I5	Number of node to which data on this card refers, i.
X(II)	D10.0	Scaled x-coordinate of node II, x_i. [L]
Y(II)	D10.0	Scaled y-coordinate of node II, y_i. [L]
THICK(II)	D10.0	Scaled thickness of mesh at node II. [L] In order to simulate radial cross-sections, set THICK(II) = (2n)(radius$_i$), where radius$_i$ is the radial distance from the vertical center axis to node II.
POR(II)	D10.0	Scaled porosity value at node II, ε_i. [1]
STOR(II)	D10.0	Scaled specific storativity value at node II, S_o, $[L^{-1}]$.

DATASET 13: Scale Factors for Elementwise Data (one card)

Variable	Format	Description
CMAXFA	D10.0	The scaled maximum hydraulic conductivity values of elements in DATASET 14 are multiplied by CMAXFA in SATRA-CHEM. May be used to convert units or to aid in assignment of maximum conductivity values in elements.
CMINFA	D10.0	The scaled minimum hydraulic conductivity values of elements in DATASET 14 are multiplied by CMINFA in SATRA-CHEM. May be used to convert units or to aid in assignment of minimum conductivity values in elements.
ANGFAC	F10.0	The scaled angles between maximum conductivity direction and x-axis of elements in DATASET 14 are multiplied by ANGFAC in SATRA-CHEM. May be used to easily assign a uniform direction of anisotropy by setting ANGFAC = angle, and all ANGLEX(L) = 1.0 in DATASET 14.
DSLFAC	D10.0	The scaled longitudinal dispersivities of elements in DATASET 14 are multiplied by DSLFAC in SATRA-CHEM. May be used to convert units or to aid in assignment of dispersivities.
DSTFAC	D10.0	The scaled transverse dispersivities of elements in DATASET 14 are multiplied by DSTFAC in SATRA-CHEM. May be used to convert units or to aid in assignment of dispersivity.

DATASET 14: Elementwise Data (one card for each of NE elements)

Variable	Format	Description
LN	I10	Number of element to which data on this card refers.
CMAX(LN)	D10.0	Scaled maximum hydraulic conductivity value of element LN, K_{max}(LN) [L/s].
CMIN(LN)	D10.0	Scaled minimum hydraulic conductivity value of element LN, K_{min}(LN). [L/s]. Isotropic conductivity requires: CMIN(LN) = CMAX(LN).
ANGLEX(LN)	F10.0	Angle measured in counterclockwise direction from +x-direction to maximum conductivity direction in element LN, θLN. [°] Arbitrary when CMIN(LN) = CMAX(LN).
DISPL(LN)	F10.0	Scaled longitudinal dispersivity value of element LN, α_L(LN) [L].
DISPT(LN)	FIO.0	Scaled transverse dispersivity value of element LN, α_T(L) [L].

DATASET 15: Optional Data for Printer Plot
(Two or three cards when plot has been requested by DATASET 7)

Variable	Format	Description
Card 1: (always required when plot is requested)		
IDIREC	I5	Chooses plot direction: Set to -1 for small plot which fits across the output page. Set to +1 for larger plot which is oriented along the output page.
NLINPI	I5	Number of printer lines per inch.
NCHAPI	I5	Number of printer characters per inch.
NCHAPL	I5	Number of printer characters per output line.
Card 2. (include this card only when pressure plots are requested in DATASET 7)		
HBASE	D13.0	Value for scaling plotted hydraulic heads. (See below.)
HDIGIT	D13.0	Digit output control for head

*The plotting routine prints three digits of the nodal value to be plotted at the (x,y) location of the node on a map of the mesh which the routine constructs. The three digits are not necessarily the first three digits of the value to be plotted, but are always one digit to the left and two digits to the right of the decimal point.

The head value to be plotted, H_{PLOT}, is calculated by SATRA-CHEM as
H_{PLOT} = (true head h_i/HBASE) (HDIGIT)
For example, HBASE may be used to scale out powers of ten and HDIGIT to shift the scaled digits of interest to the position of the three plotted digits.

Card 3: (include this card only when or concentration plots are requested in DATASET 6)

C1BASE	D13.0	Value for scaling plotted concentration C_1 values. (See below.)
C1DGIT	D13.0	Digit output control for or concentration. For explanation see (*) above. The value to be plotted, C_{PLOT}, is calculated by SATRA-CHEM as: C_{PLOT}= (concentration C_i/C2BASE)(C2DGIT) For example, CBASE may be set to the highest source concentration in the system, and CDIGIT to a value of ten; then fractional concentrations relative to the highest concentration are plotted with digits ranging from 000 to 999 which represents a relative concentration of 1.000 (~0.999).
C2BASE	D13.0	Same principle as above scaling directives.
C2DGIT	D13.0	
C4BASE	D13.0	
C4DGIT	D13.0	

DATASET 16: Optional. Data for Fluid Sources and Sinks
(one card for each of NSO source nodes as specified in DATASET 3)

Variable	Format	Description
IQC	I5	Number of node to which source/sink data on this card refers. Specifying the node number with a negative sign indicates to SATRA that the source flow rate or concentration or temperature vary in a specified manner with time. All information regarding a time-dependent source node must be programmed by the user in Subroutine BCTIME, and no other data is included on this card.
QINC	D9.0	Fluid source (or sink) which is a specified constant value at node IQC. $[L^3/s]$ A positive value is a source of fluid to the aquifer. Leave blank if IQC is negative.
C1INC C2INC C2INC	D9.0 D9.0 D9.0	Solute concentration of fluid entering the aquifer which is a specified constant value for a fluid source at node IOC. $[M_s/L^3]$ Leave blank if either IQC or QINC is negative.

DATASET 17: Optional. Data for Specified Hydraulic Head Nodes (one card for each of NHBC specified head nodes as indicated in DATASET 3, plus one blank card)

Variable	Format	Description
Cards 1 to NHBC:		
IHBC	I6	Number of node to which specified head data on this card refers. Specifying the node number with a negative sign indicates to SATRA that the specified hydraulic head value or flow concentration at this node vary in a specified manner with time. All information regarding a time-dependent specified pressure node must be programmed by the user in Subroutine BCTIME, and no other data is included on this card.
HBC	D13.0	Hydraulic head value which is a specified constant at node IHBC [L]. Leave blank if IHBC is negative.
C1BC C2BC C4BC	D13.0 D13.0 D13.0	Solute concentration of any external fluid which enters the aquifer at node IHBC. UBC is a specified constant value [M_s/L^3]. Leave blank if IHBC is negative.

Note, the last card should be blank and placed immediately following all NHBC specified head cards.

DATASET 18: Optional. Data for Specified Concentration Nodes (one card for each of NUBC nodes specified concentration nodes as indicated in DATASET 3, plus one blank card)

Variable	Format	Description
Cards 1 to NUBC.		
IC1BC IC2BC IC4BC	I6 I6 I6	Number of node to which specified concentration data on this card refers. Specifying the node number with a negative sign indicates to SATRA that the specified value at this node varies in a specified manner with time. This time-dependence must be programmed by the user in Subroutine BCTIME, and no other data is included on this card.
C1BC C2BC C4BC	D13.0 D13.0 D13.0	Concentration value in aquifer which is a specified constant at node IUBC. [M_s/L^3] Leave blank if IUBC is negative.

Note, the last card should be blank and placed immediately following the specified concentration cards.

DATASET 19: Element Incidence and Pinch Node Data
(one or two cards for each of NE elements)

Variable	Format	Description	
Card A (required for each element)			
LL	I6	Number of element to which data on this card (and the optional next card) refers. If pinch nodes exist in element LL, then the element number must be specified with a minus sign.	
Node Incidence List			
IIN(1)	I6	Number of node 1	List of corner node numbers in element LL, beginning at any node, but taken in an order counterclockwise about the element.
IIN(2)	I6	Number of node 2	
IIN(3)	I6	Number of node 3	
IIN(4)	I6	Number of node 4	

Card B (required immediately following Card A only when LL is negative)

Pinch-Node Incidence List

IEDGE(1)	I6	Node number of	IIN(1) and IIN(2)
IEDGE{2)	I6	pinch node at	IIN(2) and IIN(3}
IEDGE(3)	I6	mid-point of	IIN(3) and IIN(4)
IEDGE(4)	I6	edge between nodes:	IIN(4) and IIN(1)

A blank in the list of pinch node numbers indicates that that no node exists on that particular edge element LL.

End of Input Data List for UNIT 5

List of Input Data for UNIT 55

DATASET 1: Simulation Starting Time (One card)

Variable	Format	Description
TSTART	E20.0	Elapsed time at which the inital conditions for simulation specified in UNIT 55 are given. [s] This sets the simulation clock starting time. Usually set to a value of zero for cold-start.

DATASET 2: Initial Hydraulic Head Values at Nodes

Requires (NN + 3)/4 cards. (Done by integer arithmetic.)

Variable	Format	Description
HVEC(II)	6E13.0	Initial (starting) head values at time, TSTART, at each of NN nodes [L]. Four values per card, in exact order of node numbers. These values are arbitrary and may be left blank if the steady-state flow option in DATASET 3 of UNIT 5 has been chosen. However, the data set is still required. An initial natural head distribution for given hydrologic conditions may be obtained by running a single steady-flow time step with the store option. Then the natural heads just calculated and stored on Unit 55 file without change in format, as initial conditions for a transient run.

DATASET 3: Initial Concentration Values at Nodes

Requires (NN+3)/4 cards. (Done by integer arithmetric.)

Variable	Format	Description
C_1(II)	4D20.0	Initial (or starting) solute concentration values at time, TSTART, at each of NN nodes [M_s/L^3]. Four values per card, in exact order of node numbers.
C_2(II)	4D20.0	Initial (or at time, TSTART) solute concentration, C_2, at each of NN nodes. Four values per card in exact order of node numbers.
C_4(II)	4D20.0	Initial (or at time, TSTART) solute concentration, C_4 (or C_3), at each of NN nodes. Four values per card in exact order of node numbers.

End of Input Data List for UNIT 55

REFERENCES

Bear, Jacob, 1979, Hydraulics of groundwater: McGraw-Hill, New York, 567 p.

Bredehoeft, John D., and George F. Pinder, 1973, Mass transport in flowing groundwater: Water Resources Research, v. 9, no. 1, p. 194-210.

Cederberg, Gail A., Robert Street, and James O. Leckie, 1984, TRANQL: A groundwater mass transport and equilibrium chemistry model for multi-component systems: EOS, v. 65, no. 16, p.208.

Charbeneau, Randall J., 1981, Groundwater contaminate transport with adsorption and ion exchange chemistry: method of characteristics for the case without dispersion: Water Resources Research, v. 17, no. 3, p. 705-713.

Drever, James I., 1982, The geochemistry of natural waters: Prentice-Hall, Inc., Englewood Cliffs, N.J., 388 p.

Fetter, C. W., 1980, Applied hydrogeology: Merrill Pub. Co., Columbus, Oh., 488 p.

Freeze, Allan R., and John A. Cherry, 1979, Groundwater: Prentice-Hall, Englewood Cliffs, N.J., 604 p.

Grove, David B., and Warren W. Wood, 1979, Prediction and field verification of subsurface-water quality changes during artificial recharge, Lubbock, Texas: Groundwater, v. 17, no. 3, p. 250-257.

Gupta, Surendra P., and Robert Greenkorn, 1973, Dispersion during flow in porous media with bilinear adsorption: Water Resources Research, v. 9, no. 5, p. 1357-1368.

Holly, Donald E., and Paul R. Fenske, 1968, Transport of dissolved chemical contaminants in groundwater systems, in Nevada test site: Geological Society of America Memoir 110, E.B. Eckell Ed., p. 171-183.

Jennings, Aaron A., David J. Kirkner, and Thomas L. Theis, 1982, Multicomponent equilibrium chemistry in groundwater quality models: Water Resources Research, v. 18, no. 4, p. 1089-1096.

Konikow, Leonard F., and John D. Bredehoeft, 1974, Modeling flow and chemical quality changes in an irrigated stream-aquifer system: Water Resources Research, v. 10, no. 3, p. 546-562.

Lai, Sung-Ho, and J. J. Jurinak, 1972, Cation adsorption in one-dimensional flow through soils: a numerical solution: Water Resources Research, v. 8, no. 1, p. 99-107.

Lake, L. W., and F. Helfferich, 1978, Cation exchange in chemical flooding: part 2 - the effect of dispersion, cation exchange, and polymer/surfactant adsorption on chemical flood environment: Society of Petroleum Engineers Journal, v. 18, p. 435-444.

Miller C. W., and L. V. Benson, 1983, Simulation of solute transport in a chemically reactive heterogeneous system: model development and application: Water Resources Research, v. 19, no. 2, p. 381-391.

Parkhurst, David L., Donald C. Thorstenson, and L. Niel Plummer, 1982, PHREEQE - A computer program for geochemical calculations: U.S. Geological Survey Water Resource Investigations 80-96, 210 p.

Pickens, John F., and William Lennox, 1976, Numerical simulation of waste movement in steady groundwater flow systems: Water Resources Research, v. 12, no. 2, p. 171-180.

Pinder, George F., 1973, A Galerkin-finite element simulation of groundwater contamination on Long Island, New York: Water Resources Research, v. 9, no. 6, p. 1657-1669.

Plummer, L. Niel, Blair F. Jones, and Alfred H. Truesdell, 1978, WATEQF - A FORTRAN IV version of WATEQ, a computer program for calculating Chemical equilibrium of natural waters: U.S. Geological Survey Water Resource Investigations 76-13, 63 p.

Reardon, E. J., 1981, Kd's - can they be used to describe reversible ion sorption reactions in contaminant migration: Groundwater, v. 19, no. 3, p. 279-286.

Rubin, Jacob, 1983a, Transport of reacting solutes in porous media: relation between mathematicl nature of problem formulation and chemical nature of reactions: Water Resources Research, v. 19, no. 5, p. 1231-1252.

Rubin, Jacob, 1983b, Written communication, Research Soil Scientist with the U.S. Geological Survey, Menlo Park, California.

Rubin, Jacob, 1984, Written communication, Research Soil Scientist with the U.S. Geological Survey, Menlo Park, California.

Rubin, Jacob and R. V. James, 1973, Dispersion-affected transport of reacting solutes in saturated porous media: Galerkin method applied to equilibrium-controlled exchange in unidirectional steady water flow: Water Resources Research, v. 9, no. 5, p. 1332-1356.

Smith, G. D., 1978, Numerical solution of partial differential equations: finite difference methods: Clerendon Press, Oxford, 304 p.

Snoeyink, Vernon L., 1980, Water chemistry: John Wiley and Sons, New York, 463 p.

Strumm, W., and J. J. Morgan, 1970, Aquatic chemistry: Wiley-Interscience, New York, 83 p.

Valocchi, A. J., 1984, Validity of the local chemical equilibrium assumption for describing sorbing solute transport through homogeneous soils: EOS, v. 65, no. 16, p. 208.

Valocchi, Albert J., Robert L. Street, and Paul V. Roberts, 1981, Transport of ion-exchanging solutes in groundwater: chromatographic theory and field simulation: Water Resources Research, v. 17, no. 5, p. 1517-1527.

van Genuchten, M., and W. J. Alves, 1982, Analytical solutions of the one-dimensional convective-dispersive solute transport equation: USDA Technical Bulletin, no. 1661.

Voss, Clifford I., n.d., SATRA: A finite-element simulation model for saturated areal or cross-sectional groundwater flow and solute transport: U.S. Geological Survey Water Resource Investigations Report, in preparation, [1984].

Weast, Robert C., Melvin J. Astle, and William H. Beyer, 1983, CRC Handbook of chemistry and physics: Chemical Rubber Publishing Co.